

7 Metric-dynamic models of different varieties of «neutrinos» in the framework of the axiomatics of the Algebra of signatures

7.1 Toroidal - helical vortex in the outer shell of a moving «electron»

In the previous chapter, Chapter 6, it was shown that a simplified metric-dynamic model of the outer shell of an «electron» moving at a constant speed V_z in the direction of the z axis as a single vacuum formation relative to the vacuum extent, from which it itself consists is described by a set of metrics (6.7.1):

The outer shell of a moving «electron»

in the interval $[\sim 10^{-13} \text{ cm}, \sim 10^{18} \text{ cm}]$ with signature $(+---)$

$$ds_1^{(-a)2} = \left(1 - \frac{r_6 r}{r^2 + a_e^2 \cos^2 \theta}\right) c^2 dt^2 - \frac{r^2 + a_e^2 \cos^2 \theta}{r^2 + a_e^2 - r r_6} dr^2 - (r^2 + a_e^2 \cos^2 \theta) d\theta^2 - \left(r^2 + a_e^2 + \frac{r_6 r a_e^2 \sin^2 \theta}{r^2 + a_e^2 \cos^2 \theta}\right) \sin^2 \theta d\varphi^2 + \frac{2 r_6 r a_e}{r^2 + a_e^2 \cos^2 \theta} \sin^2 \theta d\varphi c dt. \quad - a\text{-subcont; (7.1.1)}$$

$$ds_1^{(-b)2} = \left(1 + \frac{r_6 r}{r^2 + a_e^2 \cos^2 \theta}\right) c^2 dt^2 - \frac{r^2 + a_e^2 \cos^2 \theta}{r^2 + a_e^2 + r r_6} dr^2 - (r^2 + a_e^2 \cos^2 \theta) d\theta^2 - \left(r^2 + a_e^2 - \frac{r_6 r a_e^2 \sin^2 \theta}{r^2 + a_e^2 \cos^2 \theta}\right) \sin^2 \theta d\varphi^2 + \frac{2 r_6 r a_e}{r^2 + a_e^2 \cos^2 \theta} \sin^2 \theta d\varphi c dt. \quad - b\text{-subcont. (7.1.2)}$$

The scope of a moving «electron»

in the interval $[0, \infty]$

$$ds_5^{(-)2} = c^2 dt^2 - \frac{\rho_e^2 dr^2}{r^2 + a_e^2} - \rho_e^2 d\theta^2 - (r^2 + a_e^2) \sin^2 \theta d\varphi^2, \quad (7.1.3)$$

where

$$\rho_e^2 = r^2 + a_e^2 \cos^2 \theta; \quad (7.1.4)$$

$r_6 \sim 1.7 \cdot 10^{-13} \text{ cm}$ is the radius of the «electron's» core {see hierarchy (2.6.20)};

$a_e = r_6 \frac{V_z}{2c}$ is parameter ellipticity of the moving «electron» at a constant speed V_z (in the direction of the z axis) as a single vacuum formation relative to the resting $2^3\text{-}\lambda_{m,n}$ -vacuum region, from which it consists.

Using the components of metric tensors $g_{ij}^{(-a)}$ and $g_{ij}^{(-b)}$ from metrics (7.1.1) and (7.1.2), in Chapter 6 obtained:

– components of the laminar acceleration vector of the a -subcont (or vector of a -subcont intensity $\mathbf{E}_o^{(-a)}$) (6.9.22) through (6.9.24) at the outer shell of a moving «electron»:

$$\begin{aligned}
a_{Er}^{(-a)} = E_{or}^{(-a)} &= -\gamma \frac{\partial \ln \sqrt{g_{00}^{(-a)}}}{\partial r^*} = -\frac{c^2 r_6 (a_e^2 \cos^2 \theta - r^2) (r^2 + a_e^2 - r r_6)}{2 \left(1 - \frac{r_6 r}{r^2 + a_e^2 \cos^2 \theta} \right)^{\frac{3}{2}} (r^2 + a_e^2 \cos^2 \theta)^3}, \\
a_{E\theta}^{(-a)} = E_{o\theta}^{(-a)} &= -\gamma \frac{\partial \ln \sqrt{g_{00}^{(-a)}}}{\partial \theta^*} = -\frac{c^2 r r_6 a_e^2 \sin 2\theta}{2 \left(1 - \frac{r_6 r}{r^2 + a_e^2 \cos^2 \theta} \right)^{\frac{3}{2}} (r^2 + a_e^2 \cos^2 \theta)^3}, \\
a_{E\varphi}^{(-a)} = E_{o\varphi}^{(-a)} &= -\gamma \frac{\partial \ln \sqrt{g_{00}^{(-a)}}}{\partial \varphi^*} = 0;
\end{aligned} \tag{7.1.5}$$

– components of turbulent acceleration vector of the a -subcont (6.9.28) at the outer shell of a moving «electron»:

$$\begin{aligned}
a_{Br}^{(-a)} &= (-v^{(-a)\varphi} B_{o\theta}^{(-a)}) = -\frac{v^{(-a)\varphi} c r_6 a_e \sin \theta (a_e^2 \cos^2 \theta - r^2)}{(r^2 + a_e^2 \cos^2 \theta)^{1/2} (r^2 + a_e^2 \cos^2 \theta - r_6 r)^2}, \\
a_{B\theta}^{(-a)} &= (v^{(-a)\varphi} B_{or}^{(-a)}) = -\frac{v^{(-a)\varphi} 2 c r_6 a_e \cos \theta (r^2 + a_e^2 - r_6 r)}{(r^2 + a_e^2 \cos^2 \theta)^{1/2} (r^2 + a_e^2 \cos^2 \theta - r_6 r)^2}, \\
a_{B\varphi}^{(-a)} &= (v^{(-a)r} B_{o\theta}^{(-a)} - v^{\theta(-a)} B_{or}^{(-a)}) = \frac{v^{(-a)r} c r_6 a_e \sin \theta (a_e^2 \cos^2 \theta - r^2)}{(r^2 + a_e^2 \cos^2 \theta)^{1/2} (r^2 + a_e^2 \cos^2 \theta - r_6 r)^2} + \\
&\quad + \frac{v^{(-a)\theta} 2 c r_6 a_e \cos \theta (r^2 + a_e^2 - r_6 r)}{(r^2 + a_e^2 \cos^2 \theta)^{1/2} (r^2 + a_e^2 \cos^2 \theta - r_6 r)^2};
\end{aligned} \tag{7.1.6}$$

– components of the laminar acceleration vector of the b -subcont (or vector of b -subcont intensity $\mathbf{E}_o^{(-b)}$) (6.10.6) through (6.10.8) at the outer shell of a moving «electron»:

$$a_{Er}^{(-b)} = E_{or}^{(-b)} = -\gamma \frac{\partial \ln \sqrt{g_{00}^{(-b)}}}{\partial r^*} = \frac{c^2 r_6 (a_e^2 \cos^2 \theta - r^2) (r^2 + a_e^2 + r r_6)}{2 \left(1 + \frac{r_6 r}{r^2 + a_e^2 \cos^2 \theta} \right)^{\frac{3}{2}} (r^2 + a_e^2 \cos^2 \theta)^3}, \tag{7.1.7}$$

$$a_{E\theta}^{(-b)} = E_{o\theta}^{(-b)} = -\gamma \frac{\partial \ln \sqrt{g_{00}^{(-b)}}}{\partial \theta^*} = -\frac{c^2 r r_6 a_e^2 \sin 2\theta}{2 \left(1 + \frac{r_6 r}{r^2 + a_e^2 \cos^2 \theta} \right)^{\frac{3}{2}} (r^2 + a_e^2 \cos^2 \theta)^3}, \tag{7.1.8}$$

$$a_{E\varphi}^{(-b)} = E_{o\varphi}^{(-b)} = -\gamma \frac{\partial \ln \sqrt{g_{00}^{(-b)}}}{\partial \varphi^*} = 0; \tag{7.1.9}$$

– components of turbulent acceleration vector of the b -subcont (6.10.13) at the outer shell of a moving «electron»:

$$a_{Br}^{(-b)} = \left(-v^{(-b)\varphi} B_{o\theta}^{(-b)} \right) = - \frac{v^{(-b)\varphi} c r_6 a_e \sin \theta (a_e^2 \cos^2 \theta - r^2)}{(r^2 + a_e^2 \cos^2 \theta)^{1/2} (r^2 + a_e^2 \cos^2 \theta + r_6 r)^2},$$

$$a_{B\theta}^{(-b)} = \left(v^{(-b)\varphi} B_{or}^{(-b)} \right) = - \frac{v^{(-b)\varphi} 2 c r r_6 a_e \cos \theta (r^2 + a_e^2 + r_6 r)}{(r^2 + a_e^2 \cos^2 \theta)^{1/2} (r^2 + a_e^2 \cos^2 \theta + r_6 r)^2},$$

(7.1.10)

$$a_{B\varphi}^{(-b)} = \left(v^{(-b)r} B_{o\theta}^{(-a)} - v^{\theta(-b)} B_{or}^{(-b)} \right) = \frac{v^{(-b)r} c r_6 a_e \sin \theta (a_e^2 \cos^2 \theta - r^2)}{(r^2 + a_e^2 \cos^2 \theta)^{1/2} (r^2 + a_e^2 \cos^2 \theta + r_6 r)^2} +$$

$$+ \frac{v^{(-a)\theta} 2 c r r_6 a_e \cos \theta (r^2 + a_e^2 + r_6 r)}{(r^2 + a_e^2 \cos^2 \theta)^{1/2} (r^2 + a_e^2 \cos^2 \theta + r_6 r)^2}.$$

The concept of *a-subcont* and *b-subcont* formulated in Chapter 1 (see Definition 1.7.4 and 1.7.5).

The analysis of the set of expressions (7.1.5) through (7.1.10) on the basis of mathematical methods of the Algebra of Signatures (Alsigna) (see Chapter 1 through 6) led to the following metric-dynamic model of a straight line and uniformly moving «electron» in the "vacuum" (i.e. in the 3-dimensional empty extent), stable curvature of which it is itself (see § 6.10 and § 6.11).

Around uniformly and rectilinearly moving core of the «electron» is induced toroidal-helical $a \times b$ -subcont vortex (Figure 7.1.1). In addition to the toroidal-helical vortex, there are laminar intra-vacuum flows (i.e., $a \times b$ -subcont) in the outer shell of the «electron», which flow to the «electron's» core with acceleration, and then flow away from it in the opposite direction with a slowdown (Figure 7.1.1), see § 6.11.

Thus, in the outer shell of the moving «electron», the directions of accelerated turbulent (i.e. toroidal-vortex) *a*-subcont and *b*-subcont coincide with each other, and the directions of accelerated laminar *a*-subcont

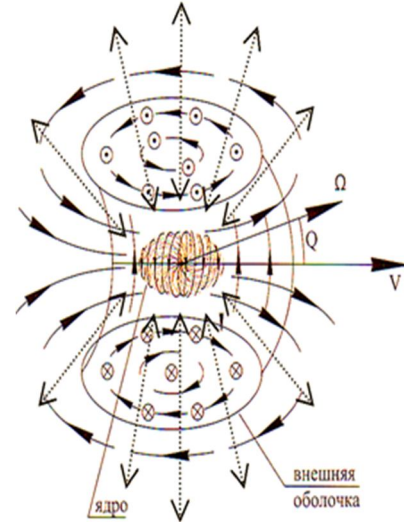


Fig. 7.1.1. Laminar and turbulent (toroidal-helical) $a \times b$ -subcont accelerated currents in the outer shell of a moving «electron»

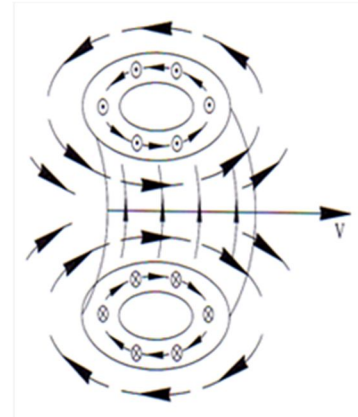


Fig. 7.1.2. Toroidal-helical vortex of the $a \times b$ -subcont without a core in its neck

and b -subcont are opposite to each other. But in any case, a -subcont and b -subcont intra-vacuum currents are intertwined with each other in double spirals (i.e. 2-braid) (see § 6.11).

7.2 The single $a \times b$ -subcont toroidal-helical vortex

Consider the possibility existence of the metric-dynamic model of single $a \times b$ -subcont toroidal-helical vortex without a core in its neck (Figure 7.1.2).

Obviously, in this vacuum formation a laminar accelerated $a \times b$ -subcont currents must be absent, since there is no core and the surrounding rakya, which is simultaneously the drain and the source of the linear intra-vacuum currents (Figure 5.10.5).

In other words, in this case, all the components of the laminar acceleration vector of the a -subcont and the laminar acceleration vector of the b -subcont should be equal to zero:

$a_{Er}^{(-a)} = E_{or}^{(-a)} = -\gamma \frac{\partial \ln \sqrt{g_{00}^{(-a)}}}{\partial r^*} = 0,$ $a_{E\theta}^{(-a)} = E_{o\theta}^{(-a)} = -\gamma \frac{\partial \ln \sqrt{g_{00}^{(-a)}}}{\partial \theta^*} = 0, \quad (7.2.1)$ $a_{E\varphi}^{(-a)} = E_{o\varphi}^{(-a)} = -\gamma \frac{\partial \ln \sqrt{g_{00}^{(-a)}}}{\partial \varphi^*} = 0.$	$a_{Er}^{(-b)} = E_{or}^{(-b)} = -\gamma \frac{\partial \ln \sqrt{g_{00}^{(-b)}}}{\partial r^*} = 0,$ $a_{E\theta}^{(-b)} = E_{o\theta}^{(-b)} = -\gamma \frac{\partial \ln \sqrt{g_{00}^{(-b)}}}{\partial \theta^*} = 0, \quad (7.2.2)$ $a_{E\varphi}^{(-b)} = E_{o\varphi}^{(-b)} = -\gamma \frac{\partial \ln \sqrt{g_{00}^{(-b)}}}{\partial \varphi^*} = 0.$
--	--

This is possible when

$$g_{00}^{(-a)} = \text{const} \quad \text{and} \quad g_{00}^{(-b)} = \text{const}. \quad (7.2.3)$$

In the case $r_6 = 0$, the metrics (7.1.1) through (7.1.2) take the form

$$ds^{(-a)2} = c^2 dt^2 - \frac{r^2 + a_e^2 \cos^2 \theta}{r^2 + a_e^2} dr^2 - (r^2 + a_e^2 \cos^2 \theta) d\theta^2 - (r^2 + a_e^2) \sin^2 \theta d\varphi^2 - a\text{-subcont}; \quad (7.2.4)$$

$$ds^{(-b)2} = c^2 dt^2 - \frac{r^2 + a_e^2 \cos^2 \theta}{r^2 + a_e^2} dr^2 - (r^2 + a_e^2 \cos^2 \theta) d\theta^2 - (r^2 + a_e^2) \sin^2 \theta d\varphi^2 - b\text{-subcont}. \quad (7.2.5)$$

and fulfilled the conditions (7.2.3).

Metrics (7.2.4) through (7.2.5) are exact solutions of Einstein's vacuum equation (2.1.6), so they describe a stable vacuum formation.

In these metrics, the parameter of ellipticity

$$a_e^2 = r_6 \frac{V_z}{2c} = r_{en} \frac{V_z}{2c} \quad (7.2.6)$$

it depends on r_6 , but in this case it is not the characteristic radius of the core of «electron» $r_6 \sim 10^{-13}$ cm, but the initial radius of the neck of the toroidal-helical vortex r_{en} , approximately equal to the characteristic radius of the «electron's» ($r_{en} \approx r_6$).

Within Alsigna the stable vacuum formation, moving with a constant velocity V_z , described by two identical metric (7.2.4) and (7.2.5) is a stable electron «neutrino»:

The stable electron «neutrino»

in the interval $[0, \infty]$ with signature $(-+++)$

$$ds^{(-a)2} = c^2 dt^2 - \frac{r^2 + a_e^2 \cos^2 \theta}{r^2 + a_e^2} dr^2 - (r^2 + a_e^2 \cos^2 \theta) d\theta^2 - (r^2 + a_e^2) \sin^2 \theta d\varphi^2 \quad -a\text{-subcont}; \quad (7.2.7)$$

$$ds^{(-b)2} = c^2 dt^2 - \frac{r^2 + a_e^2 \cos^2 \theta}{r^2 + a_e^2} dr^2 - (r^2 + a_e^2 \cos^2 \theta) d\theta^2 - (r^2 + a_e^2) \sin^2 \theta d\varphi^2 \quad -b\text{-subcont}. \quad (7.2.8)$$

The scope of a moving stable electron «neutrino»

in the interval $[0, \infty]$ with signature $(+---)$

$$ds^{(-)2} = c^2 dt^2 - dr^2 - r^2 d\theta^2 - r^2 \sin^2 \theta d\varphi^2, \quad (7.2.9)$$

where

$$a_e = r_{en} \frac{V_z}{2c} \quad (7.2.10)$$

- is the ellipticity parameter of the electron «neutrino», moving at a constant speed V_z relative to the resting $2^3\text{-}\lambda_{m,n}$ -vacuum region, the perturbation of the outer side of which it is (here r_{en} is the radius of the neck of the original toroidal-helical vortex; in the initial state, i.e. immediately after the tearing of this vortex from the «electron's» core, $r_{en} \approx r_6$).

Similar actions with metrics (6.7.9) through (6.7.10) lead to the following metric-dynamic model of positron «neutrino»

The stable positron «neutrino»

in the interval $[0, \infty]$ with signature $(-+++)$

$$ds^{(+a)2} = -c^2 dt^2 + \frac{r^2 + a_e^2 \cos^2 \theta}{r^2 + a_e^2} dr^2 + (r^2 + a_e^2 \cos^2 \theta) d\theta^2 + (r^2 + a_e^2) \sin^2 \theta d\varphi^2 \quad -a\text{-antisubcont}; \quad (7.2.11)$$

$$ds^{(+b)2} = -c^2 dt^2 + \frac{r^2 + a_e^2 \cos^2 \theta}{r^2 + a_e^2} dr^2 + (r^2 + a_e^2 \cos^2 \theta) d\theta^2 + (r^2 + a_e^2) \sin^2 \theta d\varphi^2 \quad -b\text{-antisubcont}. \quad (7.2.12)$$

The scope of a moving stable positron «neutrino»

in the interval $[0, \infty]$ with signature $(-+++)$

$$ds^{(+)} = -c^2 dt^2 + dr^2 + r^2 d\theta^2 + r^2 \sin^2 \theta d\varphi^2. \quad (7.2.13)$$

where

$$a_e = r_{en} \frac{V_z}{2c} \quad (7.2.14)$$

- is the ellipticity parameter of the positron «neutrino», moving at a constant speed V_z relative to the resting $2^3\text{-}\lambda_{m,n}$ -vacuum region, the perturbation of the inner side of which it is (here r_{en} is the radius of the neck of the original toroidal-helical vortex; in the initial state, i.e. immediately after the tearing of this vortex from the «positron's» core, $r_{en} \approx r_6$).

7.3 Deformations at the location of a stable electron «neutrino»

Consider the distortion of the «vacuum» in the area of location electron «neutrino» (7.2.7) through (7.2.9).

About deformations of «neutrino», moving at a constant speed V_z in the direction of the z axis, we will judge by the relative lengthening of the local areas of the outer side $2^3\text{-}\lambda_{m,n}$ -vacuum region {see (2.1.32)}

$$l_i^{(-)} = \sqrt{\frac{g_{ii}^{(-)}}{g_{ii}^{0(-)}}} - 1. \quad (7.3.1)$$

First, as in § 2.1 {see expressions (2.1.23) through (2.1.36)}, we find the arithmetic mean of the metric tensor component (7.2.7) and (7.2.8)

$$g_{ii}^{(-)} = \frac{1}{2} (g_{ii}^{(-a)} + g_{ii}^{(-b)}). \quad (7.3.2)$$

As a result of calculations by the formula (7.3.2), we obtain

$$\begin{aligned} g_{00}^{(-)} &= \frac{1}{2} (g_{00}^{(-a)} + g_{00}^{(-b)}) = \frac{1}{2} (1+1) = 1, \\ g_{11}^{(-)} &= \frac{1}{2} (g_{11}^{(-a)} + g_{11}^{(-b)}) = -\frac{1}{2} \left(\frac{r^2 + a_e^2 \cos^2 \theta}{r^2 + a_e^2} + \frac{r^2 + a_e^2 \cos^2 \theta}{r^2 + a_e^2} \right) = -\frac{r^2 + a_e^2 \cos^2 \theta}{r^2 + a_e^2}, \\ g_{22}^{(-)} &= \frac{1}{2} (g_{22}^{(-a)} + g_{22}^{(-b)}) = -\frac{1}{2} ((r^2 + a_e^2 \cos^2 \theta) + (r^2 + a_e^2 \cos^2 \theta)) = -(r^2 + a_e^2 \cos^2 \theta), \\ g_{33}^{(-)} &= \frac{1}{2} (g_{33}^{(-a)} + g_{33}^{(-b)}) = -\frac{1}{2} [(r^2 + a_e^2) \sin^2 \theta + (r^2 + a_e^2) \sin^2 \theta] \sin^2 \theta = -(r^2 + a_e^2) \sin^2 \theta, \end{aligned} \quad (7.3.3)$$

the rest $g_{ij}^{(-)} = 0$.

The components of the metric tensor describing the not curved condition of the investigated area of the outer side region, we take metrics the scope (7.2.9):

The components of the metric tensor $g_{ij}^{0(-)}$ describing the not curved condition of the investigated area of the outer side $2^3\text{-}\lambda_{m,n}$ -vacuum region, we take from metrics the scope (7.2.9):

$$g_{00}^{0(-)} = 1, \quad g_{11}^{0(-)} = -1, \quad g_{22}^{0(-)} = -r^2, \quad g_{33}^{0(-)} = -r^2 \sin^2 \theta. \quad (7.3.4)$$

Substituting the components (7.3.3) and (7.3.4) into the expression (7.3.1), we obtain the following components of the vector of the relative lengthening of the subcont:

$$l_t^{(-)} = \sqrt{\frac{1}{1}} - 1 = 0, \quad (7.3.5)$$

$$l_r^{(-)} = \sqrt{\frac{r^2 + a_e^2 \cos^2 \theta}{r^2 + a_e^2}} - 1 = \sqrt{\frac{r^2 + (r_6 \frac{V_z}{2c})^2 \cos^2 \theta}{r^2 + (r_6 \frac{V_z}{2c})^2}} - 1, \quad (7.3.6)$$

$$l_\theta^{(-)} = \sqrt{1 + \frac{a_e^2 \cos^2 \theta}{r^2}} - 1 = \sqrt{1 + \frac{(r_6 \frac{V_z}{2c})^2 \cos^2 \theta}{r^2}} - 1, \quad (7.3.7)$$

$$l_\varphi^{(-)} = \sqrt{1 + \frac{a_e^2}{r^2}} - 1 = \sqrt{1 + \frac{(r_6 \frac{V_z}{2c})^2}{r^2}} - 1. \quad (7.3.8)$$

Function graphs (7.3.5) through (7.3.8) are shown in Figures 7.3.1 through 7.3.3

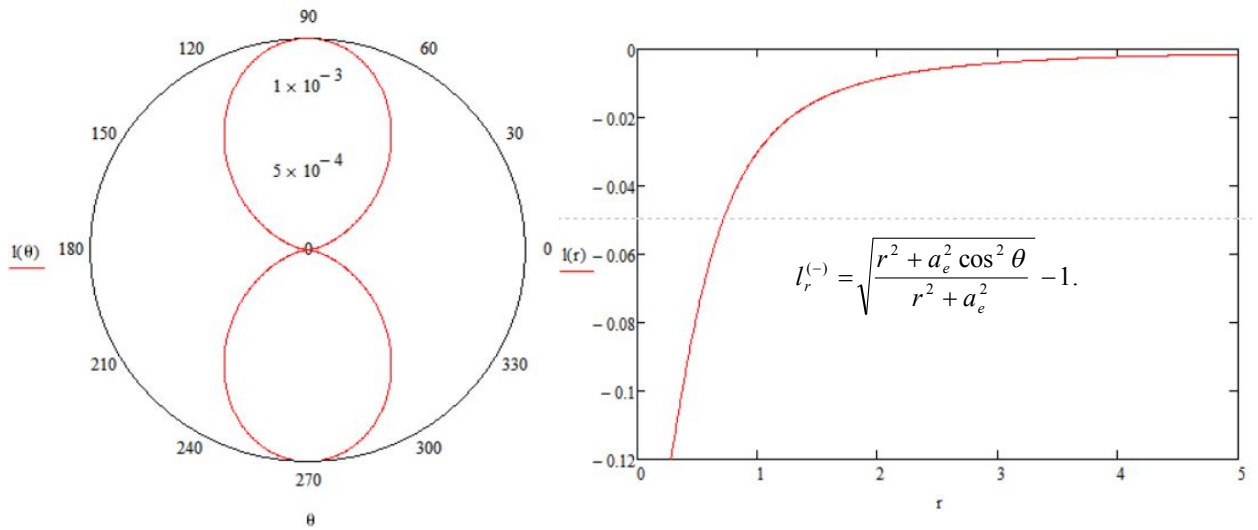


Fig. 7.3.1. Function graphs (7.3.6) for $r = 10$, $a_e = 0.5$, $\theta = 10$

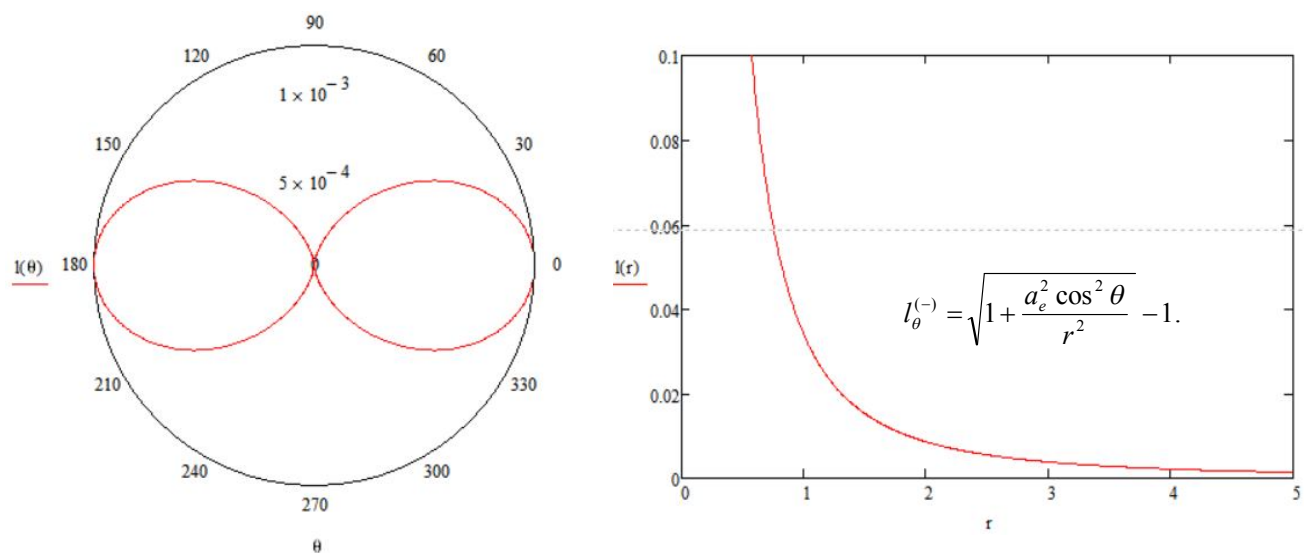


Fig. 7.3.2. Function graphs (7.3.7) for $r = 10$, $a_e = 0.5$, $\theta = 10$

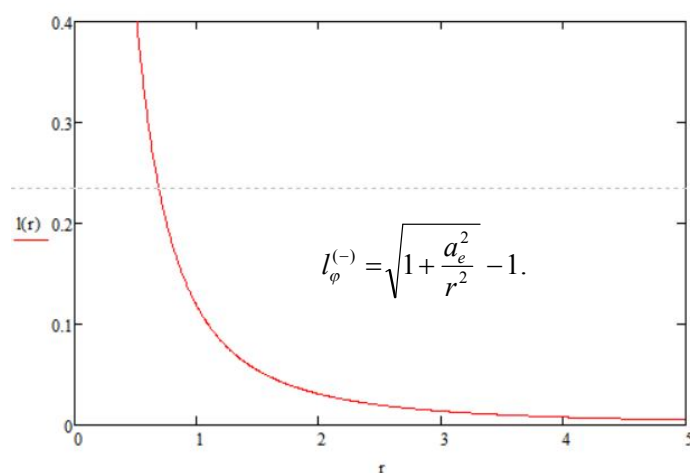


Fig. 7.3.3. The graph of the function (7.3.8) with $a_e = 0.5$. The calculations are performed using the MathCad software

Analysis of function graphs (7.3.5) through (7.3.8) leads to the conclusion that a stable electron «neutrino» is a toroidal deformation of the subcont (i.e., the outer side 2^3 - $\lambda_{m,n}$ -vacuum region, see *table. 6.2.1*), which is moved with a constant speed V_z in the direction of the z axis.

For Figure 7.3.4 various attempts are made to illustrate the distortion of the subcont in the vicinity of the location of the center of a stable electron «neutrino».

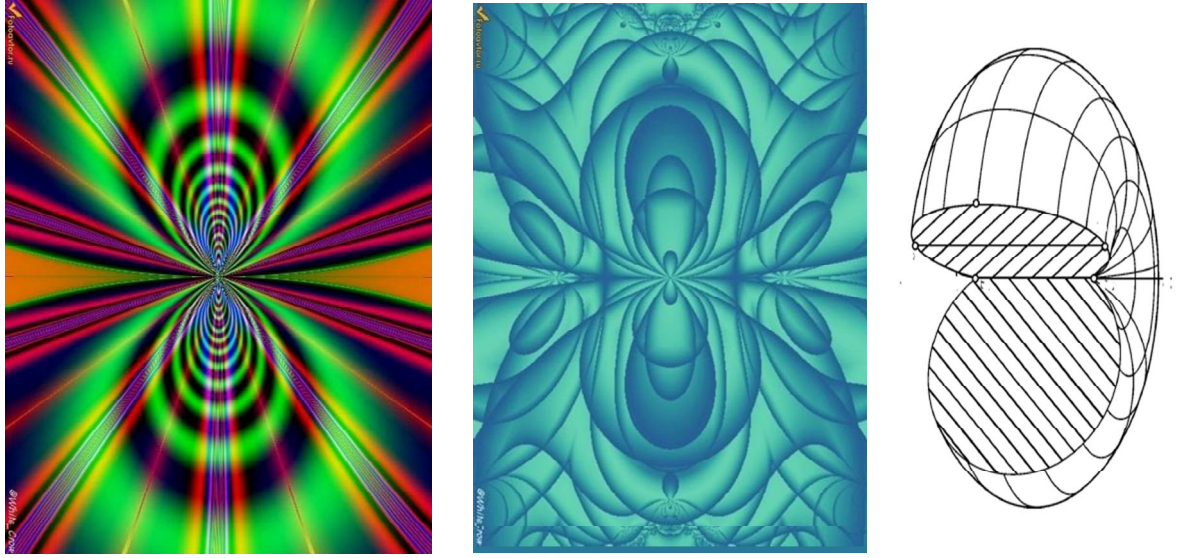


Fig. 7.3.4. Attempts to illustrate the distortions of the outer side of $2^3\text{-}\lambda_{m,n}$ -vacuum region in the vicinity of the location of the center of a stable electron «neutrino»

Analysis of the metrics (7.2.7) through (7.2.8) and relative lengthening (7.3.5) through (7.3.8) shows that at $a_e = 0$ (in the particular case when $V_z = 0$) the curvature of the outer side $2^3\text{-}\lambda_{m,n}$ -vacuum region smoothed and electron «neutrino» disappear. That is, electron «neutrinos» cannot exist without translational motion at a certain speed V_z .

Metrics (7.2.7) through (7.2.8) defining the metric-dynamic properties of an electron «neutrino» remain unchanged as long as the ellipticity parameter a_e (7.2.10) remains constant

$$a_e = r_{en} \frac{V_z}{2c} = \text{const}.$$

The a_e parameter can remain constant in three cases:

- 1) V_z and r_{en} are unchanged, so that $a_e = \text{const}$;
- 2) V_z is reduced, while r_{en} is proportionally increased, so that $a_e = \text{const}$;
- 3) V_z increases, with r_{en} decreasing proportionally, so that $a_e = \text{const}$.

In the second case, if V_z decreases to zero, then r_{en} increases to infinity. This is similar to the toroidal smoke rings in the air, which, as they move away from their place of origin, gradually slow down and expand to complete dissolution (Figure 7.3.5).



Fig. 7.3.5. A smoke toroidal-helical ring as the distance from the place of their occurrence gradually slow down and expand (<https://www.slrlounge.com>)

In the third case, if r_{en} is reduced to zero, then V_z is increased to infinity.

Indeed, from expressions (7.2.8) through (7.2.9) and (7.3.5) through (7.3.8) it follows that there are no formal restrictions on the travel speed of a stable electron «neutrino» V_z . Since a zero components of the metric tensors of the metrics (7.2.7) and (7.2.8) is equal to

$$g_{00}^{(-a)} = 1, \quad g_{01}^{(-a)} = 0, \quad g_{02}^{(-a)} = 0, \quad g_{03}^{(-a)} = 0, \quad (7.3.9)$$

$$g_{00}^{(-b)} = 1, \quad g_{01}^{(-b)} = 0, \quad g_{02}^{(-b)} = 0, \quad g_{03}^{(-b)} = 0, \quad (7.3.10)$$

obtain

$$g_r^{(-a)} = -\frac{g_{01}^{(-a)}}{g_{00}^{(-a)}} = 0, \quad g_\theta^{(-a)} = -\frac{g_{02}^{(-a)}}{g_{00}^{(-a)}} = 0, \quad g_\varphi^{(-a)} = -\frac{g_{03}^{(-a)}}{g_{00}^{(-a)}} = 0; \quad (7.3.11)$$

$$g_r^{(-b)} = -\frac{g_{01}^{(-b)}}{g_{00}^{(-b)}} = 0, \quad g_\theta^{(-b)} = -\frac{g_{02}^{(-b)}}{g_{00}^{(-b)}} = 0, \quad g_\varphi^{(-b)} = -\frac{g_{03}^{(-b)}}{g_{00}^{(-b)}} = 0 \quad (7.3.12)$$

and, therefore, this local vacuum formation does not have any accelerated laminar and turbulent intra-vacuum currents:

$B_{or}^{(-a)} = \frac{\gamma \sqrt{g_{00}^{(-a)}}}{2c \sqrt{ g }} \left(\frac{\partial g_{\phi}^{(-a)}}{\partial \theta} - \frac{\partial g_{\theta}^{(-a)}}{\partial \phi} \right) = 0,$ $B_{o\theta}^{(-a)} = \frac{\gamma \sqrt{g_{00}^{(-a)}}}{2c \sqrt{ g }} \left(\frac{\partial g_r^{(-a)}}{\partial \phi} - \frac{\partial g_{\phi}^{(-a)}}{\partial r} \right) = 0, \quad (7.3.14)$ $B_{o\phi}^{(-a)} = \frac{\gamma \sqrt{g_{00}^{(-a)}}}{2c \sqrt{ g }} \left(\frac{\partial g_{\theta}^{(-a)}}{\partial r} - \frac{\partial g_r^{(-a)}}{\partial \theta} \right) = 0.$	$E_{or}^{(-a)} = -\gamma \frac{\partial \ln \sqrt{g_{00}^{(-a)}}}{\partial r^*} = 0,$ $E_{o\theta}^{(-a)} = -\gamma \frac{\partial \ln \sqrt{g_{00}^{(-a)}}}{\partial \theta^*} = 0, \quad (7.3.13)$ $E_{o\phi}^{(-a)} = -\gamma \frac{\partial \ln \sqrt{g_{00}^{(-a)}}}{\partial \phi^*} = 0.$
<div style="display: flex; justify-content: space-around; align-items: center;"> <div style="text-align: center;">H V</div> <div style="text-align: center;">I H</div> </div>	
$E_{or}^{(-b)} = -\gamma \frac{\partial \ln \sqrt{g_{00}^{(-b)}}}{\partial r^*} = 0,$ $E_{o\theta}^{(-b)} = -\gamma \frac{\partial \ln \sqrt{g_{00}^{(-b)}}}{\partial \theta^*} = 0, \quad (7.3.15)$ $E_{o\phi}^{(-b)} = -\gamma \frac{\partial \ln \sqrt{g_{00}^{(-b)}}}{\partial \phi^*} = 0.$	$B_{or}^{(-b)} = \frac{\gamma \sqrt{g_{00}^{(-b)}}}{2c \sqrt{ g }} \left(\frac{\partial g_{\phi}^{(-b)}}{\partial \theta} - \frac{\partial g_{\theta}^{(-ab)}}{\partial \phi} \right) = 0,$ $B_{o\theta}^{(-b)} = \frac{\gamma \sqrt{g_{00}^{(-b)}}}{2c \sqrt{ g }} \left(\frac{\partial g_r^{(-b)}}{\partial \phi} - \frac{\partial g_{\phi}^{(-b)}}{\partial r} \right) = 0, \quad (7.3.16)$ $B_{o\phi}^{(-b)} = \frac{\gamma \sqrt{g_{00}^{(-a)}}}{2c \sqrt{ g }} \left(\frac{\partial g_{\theta}^{(-b)}}{\partial r} - \frac{\partial g_r^{(-b)}}{\partial \theta} \right) = 0.$

Therefore, within Alsigna the stable electron «neutrino» (7.2.7) through (7.2.9) don't have any inert properties. In other words, we come to the need to consider the hypothesis that stable electron «neutrinos» (toroidal vacuum "ghosts" or "phantoms") described by a set of metrics (7.2.7) through (7.2.9) don't possess inertia, and therefore they can move in a "vacuum" at a speed many times greater than the speed of light ($V_z \gg c$).

If we learn how to generate and detect such superluminal non-inertial stable vacuum formations, then tasks can be set for the organization of narrow-directional communication channels with the speed of data transmission significantly exceeding the speed of light.

7.4 The possibility of formation of electron «neutrinos»

Suppose that a solid obstacle has arisen in the path of the «electron's» core moving at a velocity V_z , whose outer shell is described by a set of metrics (7.1.1) through (7.1.2) (Figure 7.4.1).

Let us assume that as a result of the collision of the core with this obstacle, it abruptly stops and restores the original spherical shape and the field of the vector of $a \times b$ -subcont intensity $\mathbf{E}_o^{(-)}$ (Figure 7.4.1). At the same time, the toroidal-helical motion of the outer shell of the moving «electron» due to inertia flies off its stopped core, and continues to move in the form of a toroidal-helical vortex in the same direction and at the same initial velocity V_z (Figure 7.4.1).

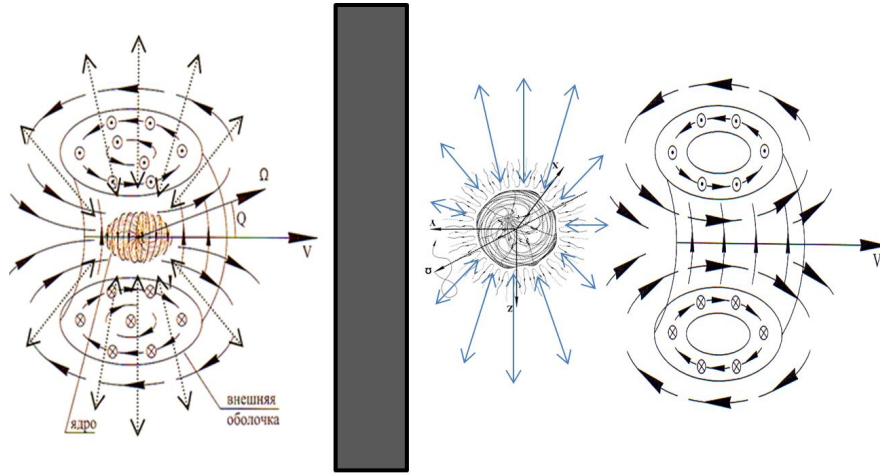


Fig. 7.4.1. Moving «electron», faced with a solid obstacle, is divided into a resting «electron» and a separate toroidal-helical vortex (i.e. the initial state of the electron «neutrino»), which continues to move at a speed $V=V_z$

It should be expected that the toroidal-helical vortex, which fled off from the core of the stopped «electron», is the initial state of the electron «neutrino». The metric-dynamic model of such a «neutrino» can be obtained from metrics (7.1.1) and (7.1.2) by equating zero components of the metric tensor with one:

$$g_{00}^{(-a)} = 1, \quad g_{00}^{(-b)} = 1,$$

since the toroidal-helical vortex, due to the loss of the core, there should be no accelerated laminar flows described by $a \times b$ -subcont intensity $E_o^{(-)}$ (6.11.5) with a set of components (7.1.5) and (7.1.7) through (7.1.9).

Under the conditions of (7.4.4), the metric (7.1.1) through (7.1.2) we get the following set of metrics:

The initial state of the electron «neutrinos»

in the interval $[\sim 10^{-13} \text{ cm}, \sim 10^{18} \text{ cm}]$ with signature $(+---)$

$$ds_1^{(-a)2} = c^2 dt^2 - \frac{r^2 + a_e^2 \cos^2 \theta}{r^2 + a_e^2 - rr_{en}} dr^2 - (r^2 + a_e^2 \cos^2 \theta) d\theta^2 -$$

$$- \left(r^2 + a_e^2 + \frac{r_{en} r a_e^2 \sin^2 \theta}{r^2 + a_e^2 \cos^2 \theta} \right) \sin^2 \theta d\varphi^2 + \frac{2r_{en} r a_e}{r^2 + a_e^2 \cos^2 \theta} \sin^2 \theta d\varphi c dt. \quad -a\text{-subcont; } (7.4.1)$$

$$ds_1^{(-b)2} = c^2 dt^2 - \frac{r^2 + a_e^2 \cos^2 \theta}{r^2 + a_e^2 + rr_{en}} dr^2 - (r^2 + a_e^2 \cos^2 \theta) d\theta^2 -$$

$$- \left(r^2 + a_e^2 - \frac{r_{en} r a_e^2 \sin^2 \theta}{r^2 + a_e^2 \cos^2 \theta} \right) \sin^2 \theta d\varphi^2 + \frac{2r_{en} r a_e}{r^2 + a_e^2 \cos^2 \theta} \sin^2 \theta d\varphi c dt. \quad -b\text{-subcont } (7.4.2)$$

The scope of initial state electron «neutrino»

in the interval $[0, \infty]$

$$ds_5^{(-)2} = c^2 dt^2 - \frac{(r^2 + a_e^2 \cos^2 \theta) dr^2}{r^2 + r^2 + a_e^2 \cos^2 \theta} - (r^2 + a_e^2 \cos^2 \theta) d\theta^2 - (r^2 + a_e^2) \sin^2 \theta d\varphi^2, \quad (7.4.3)$$

where
$$a_e = r_{en} \frac{V_z}{2c} \quad (7.4.4)$$

- is the ellipticity parameter of the toroidal-helical vortex moving with the velocity V_z (in the direction of the z axis) with the initial radius of the neck $r_{en} \approx r_6$.

That is the vacuum formation described by the metrics (7.4.1) and (7.4.2) has all the components of the vector of a -subcont intensity $\mathbf{E}_o^{(-a)}$ and of the vector of b -subcont intensity $\mathbf{E}_o^{(-b)}$ equal to zero {see (7.2.1) and (7.2.2)}. At the same time, as shown in §§ 6.9 through 6.10, we have:

- components of the turbulent acceleration vector a -subcont in the initial state of the electron «neutrino»

$$a_{Br}^{(-a)} = \left(-v^{(-a)\varphi} B_{o\theta}^{(-a)} \right) = - \frac{v^{(-a)\varphi} c r_{en} a_e \sin \theta (a_e^2 \cos^2 \theta - r^2)}{(r^2 + a_e^2 \cos^2 \theta)^{1/2} (r^2 + a_e^2 \cos^2 \theta - r_{en} r)^2},$$

$$a_{B\theta}^{(-a)} = \left(v^{(-a)\varphi} B_{or}^{(-a)} \right) = - \frac{v^{(-a)\varphi} 2 c r_{en} a_e \cos \theta (r^2 + a_e^2 - r_{en} r)}{(r^2 + a_e^2 \cos^2 \theta)^{1/2} (r^2 + a_e^2 \cos^2 \theta - r_{en} r)^2}, \quad (7.4.5)$$

$$a_{B\varphi}^{(-a)} = \left(v^{(-a)r} B_{o\theta}^{(-a)} - v^{\theta(-a)} B_{or}^{(-a)} \right) = \frac{v^{(-a)r} c r_{en} a_e \sin \theta (a_e^2 \cos^2 \theta - r^2)}{(r^2 + a_e^2)^{1/2} (r^2 + a_e^2 \cos^2 \theta - r_{en} r)^2} +$$

$$+ \frac{v^{(-a)\theta} 2 c r_{en} a_e \cos \theta (r^2 + a_e^2 - r_{en} r)}{(r^2 + a_e^2 \cos^2 \theta)^{1/2} (r^2 + a_e^2 \cos^2 \theta - r_{en} r)^2},$$

- is components of the turbulent acceleration vector b -subcont in the initial state of motion of the electron «neutrino».

$$a_{Br}^{(-b)} = \left(-v^{(-b)\varphi} B_{o\theta}^{(-b)} \right) = - \frac{v^{(-b)\varphi} c r_{en} a_e \sin \theta (a_e^2 \cos^2 \theta - r^2)}{(r^2 + a_e^2 \cos^2 \theta)^{1/2} (r^2 + a_e^2 \cos^2 \theta + r_6 r)^2},$$

$$a_{B\theta}^{(-b)} = \left(v^{(-b)\varphi} B_{or}^{(-b)} \right) = - \frac{v^{(-b)\varphi} 2 c r r_{en} a_e \cos \theta (r^2 + a_e^2 + r_{en} r)}{(r^2 + a_e^2 \cos^2 \theta)^{1/2} (r^2 + a_e^2 \cos^2 \theta + r_{en} r)^2}, \quad (7.4.6)$$

$$a_{B\varphi}^{(-b)} = \left(v^{(-b)r} B_{o\theta}^{(-b)} - v^{\theta(-b)} B_{or}^{(-b)} \right) = \frac{v^{(-b)r} c r_{en} a_e \sin \theta (a_e^2 \cos^2 \theta - r^2)}{(r^2 + a_e^2 \cos^2 \theta)^{1/2} (r^2 + a_e^2 \cos^2 \theta + r_{en} r)^2} +$$

$$+ \frac{v^{(-b)\theta} 2 c r r_{en} a_e \cos \theta (r^2 + a_e^2 + r_6 r)}{(r^2 + a_e^2 \cos^2 \theta)^{1/2} (r^2 + a_e^2 \cos^2 \theta + r_{en} r)^2}.$$

Together, components (7.4.5) and (7.4.6) describe the initial state of $a \times b$ -subcont toroidal-helical vortex (Figure 7.4.2 a).

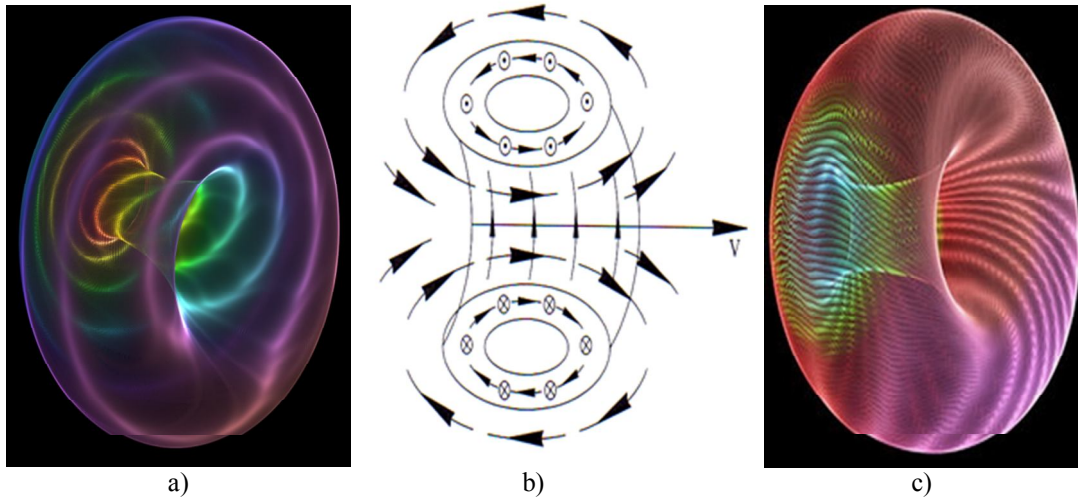


Fig. 7.4.2. Illustration of the dynamics of $a \times b$ -subcont toroidal-helical vortex, which is called an electron «neutrino» in the framework of the Alsigna

It is obvious that the metrics (7.4.1) and (7.4.2) are not solutions of the Einstein vacuum equation (2.1.6) (as can be seen by substituting the components of the metric tensor from these metrics into this equation). This means that the metrics (7.4.1) and (7.4.2) cannot describe stable vacuum formation, as laminar accelerations of intra-vacuum layers are eliminated, so there is no complete compensation of intra-vacuum deformations.

It is natural to assume that an unstable $a \times b$ -subcont toroidal-helical vortex, which is described by metrics (7.4.1) through (7.4.2) (Figure 7.4.2 a), evolves into a stable vacuum formation as described by the metrics (7.2.7) through (7.2.8) as it moves towards the z axis.

Evolution of metrics (7.4.2) through (7.4.4) into metrics (7.2.7) through (7.2.8) is possible only due to gradual reduction of the neck radius r_{en} of the toroidal-helical vortex to zero ($r_{en} \rightarrow 0$).

When the radius of the neck of the toroidal-helical vortex r_{en} decreases, the ellipticity parameter $a_e = r_{en}V_z/(2c)$ can remain constant only if its velocity V_z increases in proportion to the reduction r_{en} .

In this case, the increase in the velocity of «neutrino» motion of V_z can be explained by the reversal of the rotational motion of the toroidal-helical vortex in the acceleration of its translational motion, i.e. by maintaining the balance of the total amount of motion.

At the same time, the scope of the initial state of the electron «neutrino» (7.4.3) evolves into the scope of its finite stable state (7.2.9) by gradually increasing r_{en} to infinity (i.e. alignment) and proportional reduction of V_z to zero, while the ellipticity parameter a_e remains constant.

At a great distance from the neck (i.e. at $r \gg r_{en}$) the components of the turbulent acceleration vector a -subcont (7.4.5) and b -subcont (7.4.6) are simplified:

$a_{Br}^{(-a)} = \frac{v^{(-a)\varphi} c r_{en} a_e \sin \theta}{r^3} = \frac{v^{(-a)\varphi} r_{en}^2 V_z \sin \theta}{2r^3},$ $a_{B\theta}^{(-a)} = -\frac{v^{(-a)\varphi} 2c r_{en} a_e \cos \theta}{r^2} = -\frac{v^{(-a)\varphi} r_{en}^2 V_z \cos \theta}{r^2},$ $a_{B\varphi}^{(-a)} = \frac{v^{(-a)\theta} 2c r_{en} a_e \cos \theta}{r^2} = \frac{v^{(-a)\theta} r_{en}^2 V_z \cos \theta}{r^2}.$ <p style="text-align: right;">(7.4.7)</p>	$a_{Br}^{(-b)} = \frac{v^{(-b)\varphi} c r_{en} a_e \sin \theta}{r^3} = \frac{v^{(-b)\varphi} r_{en}^2 V_z \sin \theta}{2r^3},$ $a_{B\theta}^{(-b)} = -\frac{v^{(-b)\varphi} 2c r_{en} a_e \cos \theta}{r^2} = -\frac{v^{(-b)\varphi} r_{en}^2 V_z \cos \theta}{r^2},$ $a_{B\varphi}^{(-b)} = \frac{v^{(-b)\theta} 2c r_{en} a_e \cos \theta}{r^2} = \frac{v^{(-b)\theta} r_{en}^2 V_z \cos \theta}{r^2}.$ <p style="text-align: right;">(7.4.8)</p>
--	--

The components of the acceleration vector of the subcont, according to (5.7.2), are equal

$$a_{Br}^{(-)} = a_{Br}^{(-a)} + i a_{Br}^{(-b)},$$

$$a_{B\theta}^{(-)} = a_{B\theta}^{(-a)} + i a_{B\theta}^{(-b)}, \quad (7.4.9)$$

$$a_{B\varphi}^{(-)} = a_{B\varphi}^{(-a)} + i a_{B\varphi}^{(-b)}.$$

Substituting the components of (7.4.7) and (7.4.8) in the expression (7.4.9), receive

$$a_{Br}^{(-)} = \left(a_{Br}^{(-a)2} + a_{Br}^{(-b)2} \right)^{1/2} = \frac{\sqrt{2} v^{(-a)\varphi} r_{en}^2 V_z \sin \theta}{2r^2},$$

$$a_{B\theta}^{(-)} = \left(a_{B\theta}^{(-a)2} + a_{B\theta}^{(-b)2} \right)^{1/2} = -\frac{\sqrt{2} v^{(-a)\varphi} r_{en}^2 V_z \cos \theta}{r^2}, \quad (7.4.10)$$

$$a_{B\varphi}^{(-)} = \left(a_{B\varphi}^{(-a)2} + a_{B\varphi}^{(-b)2} \right)^{1/2} = \frac{\sqrt{2} v^{(-a)\theta} r_{en}^2 V_z \cos \theta}{r^2}.$$

Where it is clear that the accelerated (rotational) movement of subcont at a great distance from the neck of the toroidal-helical vortex can be increased by increasing the speed of the translational motion of the vortex V_z , or increase the radius of his neck r_{en} .

Within Alsinga consider $a \times b$ -subcount toroidal-helical vortex, the described components of the vectors of the turbulent acceleration of a -subcont (7.4.5) and b -subcont (7.4.6), is a closed accelerated flow of the various layers of the outer part $2^3\text{-}\lambda_{m,n}$ -vacuum region. From the point of view of classical electrodynamics, this initial state of electron «neutrinos» is a magnetic monopole, whose power lines are self-closed.

7.5 Possibility generating of an aquatic «neutrino». Volkov impact effect

Alsinga admits the existence not only of electron and positron «neutrinos». The existence of the «neutrino» on a much larger scale is also possible.

The employee of Moscow State University Y. V. Volkov placed the ampoule with double-distilled water (bidistillate) for two weeks in a powerful magnetic field with induction ~ 0.5 Tesla. Further, Volkov observed the following effects:

- the weight of the ampoule with magnetized double-distilled water was increased by $\sim 2,2 \cdot 10^{-4}$ g;
- when on ampoule with magnetized double-distilled water were directed beam of red light (i.e. the beam of a common laser pointer), then the added weight of water was lost within 1.5 to 2.5 minutes;
- ampoule with magnetized double-distilled water placed on a styrofoam raft on the water surface, moving in the direction of the source of the red beam of light (Figure 7.5.1);

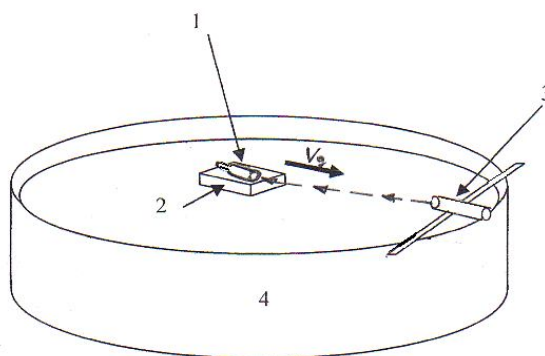


Fig. 7.5.1. The Volkov impact effect is the movement of the ampoule with magnetized water in the direction of the source of red light (i.e. laser pointers):

- 1 – ampoule with a magnetic double-distilled water;
- 2 – styrofoam raft on the water surface;
- 3 – laser pointer illuminating the bottom of the ampoule;
- 4 – a bowl of water.

– the demagnetization of double-distilled water by means of a red light beam having radiation (not clear nature) in the same direction, which was directed beam laser pointer. This strange radiation had a high penetrating power. Y. V. Volkov put on the path of propagation of the beam of a red laser passing through a vial of magnicent distillate, various solid objects. The obstacles do not miss the laser beam. However, the spectrometer installed behind the barriers, recorded the flow of strange radiation, so intense that the sensing element of the device failed.

For explanation of Y. V. Volkov experiments with magnetized water Alsigna proposed the following hypothesis [11].

Many experiments conducted by different groups of researchers speak about the cluster structure of water (see, for example, [26]). Under water clusters the associated state of about two billion water molecules is mainly formed.

Water clusters appear, for example, when water is irradiated with coherent light sources. For Figure 7.5.2 the results of such experiments are presented. The sizes of water clusters are estimated in the order $\sim 5 \cdot 10^{-6}$ cm.

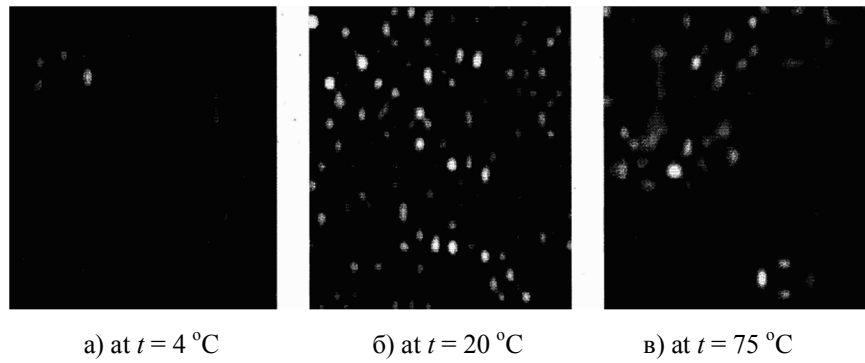


Fig. 7.5.2. Cluster structure of water. The typical size of the water cluster $\sim 5 \cdot 10^{-6}$ cm
Photo submitted by A. N. Smirnov

Alsigna believes that with the long-term presence of distilled water under the influence of a powerful magnetic field, its clusters are deformed, and around them there is a rotation of the vacuum layers, i.e. a magnetic field is induced (Figure 7.5.3).

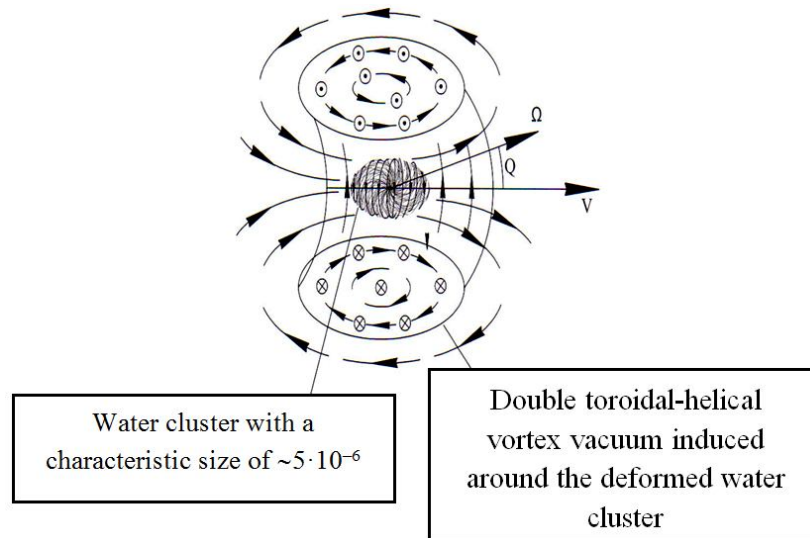


Fig. 7.5.3. Rotational movement of the vacuum around the deformed water cluster

The wavelength of red light $\lambda = 0.6$ through $0.65 \mu\text{m} \approx 6.5 \cdot 10^{-5}$ cm are commensurable with the sizes magnetized water clusters. Therefore, the laser beam can stimulate the jump off of an intra-vacuum double toroidal-helical vortex from water clusters (Figure 7.5.4).

At the same time, the breaking vortices repel water clusters in the opposite direction, thus offering an explanation of the Volkov impact effect (Figure 7.5.1).

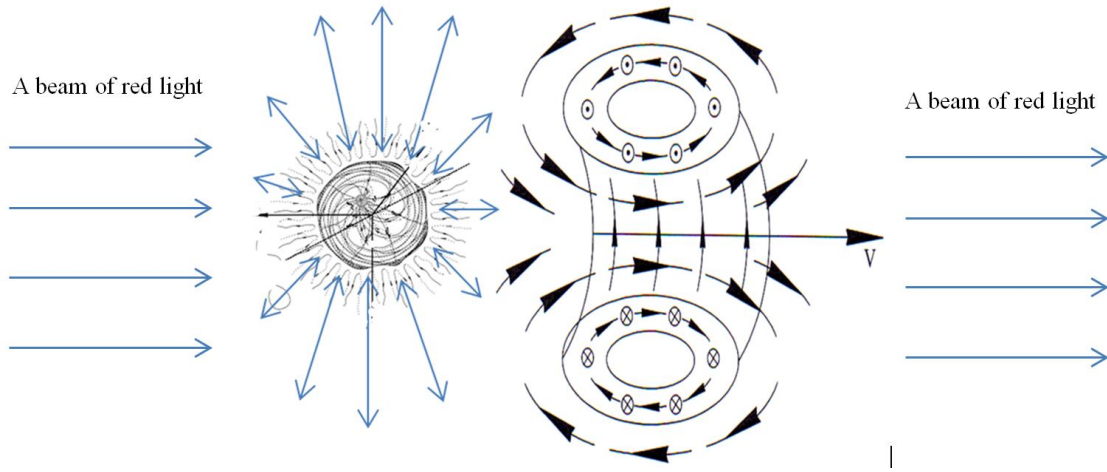


Fig. 7.5.4. Vacuum toroidal-helical vortex flies from the water cluster with a characteristic size $\sim 5 \cdot 10^{-6}$ cm

Water clusters are electrically neutral, because both positively and negatively charged particles are located inside the cluster. Therefore, within the framework of the Alsigna, the averaged metric-dynamic model of the initial state (i.e., the aquatic «neutrino» that has just flies from the water cluster) is described by four metrics (7.4.1) through (7.4.2):

The initial state of the aquatic «neutrino»

in the interval $[\sim 10^{-5} \text{ cm}, \sim 10^{18}]$ with signature $2(+ --) + 2(- ++)$

$$ds_1^{(-a)2} = c^2 dt^2 - \frac{r^2 + a_w^2 \cos^2 \theta}{r^2 + a_w^2 - rr_{en}} dr^2 - (r^2 + a_w^2 \cos^2 \theta) d\theta^2 -$$

– *a*-subcont; (7.5.1)

$$- \left(r^2 + a_w^2 + \frac{r_{en} r a_w^2 \sin^2 \theta}{r^2 + a_w^2 \cos^2 \theta} \right) \sin^2 \theta d\varphi^2 + \frac{2r_{en} r a_w}{r^2 + a_w^2 \cos^2 \theta} \sin^2 \theta d\varphi c dt.$$

$$ds_2^{(-b)2} = c^2 dt^2 - \frac{r^2 + a_w^2 \cos^2 \theta}{r^2 + a_w^2 + rr_{en}} dr^2 - (r^2 + a_w^2 \cos^2 \theta) d\theta^2 -$$

– *b*-subcont; (7.5.2)

$$- \left(r^2 + a_w^2 - \frac{r_{en} r a_w^2 \sin^2 \theta}{r^2 + a_w^2 \cos^2 \theta} \right) \sin^2 \theta d\varphi^2 + \frac{2r_{en} r a_w}{r^2 + a_w^2 \cos^2 \theta} \sin^2 \theta d\varphi c dt.$$

$$ds_3^{(+a)2} = -c^2 dt^2 + \frac{r^2 + a_w^2 \cos^2 \theta}{r^2 + a_w^2 - rr_{en}} dr^2 + (r^2 + a_w^2 \cos^2 \theta) d\theta^2 +$$

– *a*-antisubcont; (7.5.3)

$$+ \left(r^2 + a_w^2 + \frac{r_{en} r a_w^2 \sin^2 \theta}{r^2 + a_w^2 \cos^2 \theta} \right) \sin^2 \theta d\varphi^2 - \frac{2r_{en} r a_w}{r^2 + a_w^2 \cos^2 \theta} \sin^2 \theta d\varphi c dt.$$

$$ds_4^{(+b)2} = -c^2 dt^2 - \frac{r^2 + a_w^2 \cos^2 \theta}{r^2 + a_w^2 + rr_{en}} dr^2 + (r^2 + a_w^2 \cos^2 \theta) d\theta^2 +$$

– *b*-sntyisubcont. (7.5.4)

$$+ \left(r^2 + a_w^2 - \frac{r_{en} r a_w^2 \sin^2 \theta}{r^2 + a_w^2 \cos^2 \theta} \right) \sin^2 \theta d\varphi^2 - \frac{2r_{en} r a_w}{r^2 + a_w^2 \cos^2 \theta} \sin^2 \theta d\varphi c dt.$$

The scope of initial state of the aquatic «neutrino»

in the interval $[0, \infty]$ with signature $(+ - -) + (- + +)$

$$ds_5^{(\pm)2} = ds_5^{(-)2} + ds_5^{(+)2}. \quad (7.5.5)$$

where

$$ds_5^{(-)2} = c^2 dt^2 - \frac{(r^2 + a_w^2 \cos^2 \theta) dr^2}{r^2 + r^2 + a_w^2 \cos^2 \theta} - (r^2 + a_w^2 \cos^2 \theta) d\theta^2 - (r^2 + a_w^2) \sin^2 \theta d\varphi^2,$$

$$ds_5^{(+)2} = -c^2 dt^2 + \frac{(r^2 + a_w^2 \cos^2 \theta) dr^2}{r^2 + r^2 + a_w^2 \cos^2 \theta} + (r^2 + a_w^2 \cos^2 \theta) d\theta^2 + (r^2 + a_w^2) \sin^2 \theta d\varphi^2,$$

where $a_w = r_{wn} \frac{V_z}{2c}$ is the ellipticity parameter of a double toroidal-helical vortex (aquatic «neutrino») moving at a speed V_z (in the direction of the z axis) with an initial neck radius $r_{wn} \sim 5 \cdot 10^{-6}$ cm.

The neck of the aquatic «neutrino» is about seven orders of magnitude larger than the neck of the electron «neutrino», since $r_{wn} / r_{en} \approx 10^{-6} / 10^{-13} \sim 10^7$ (Figure 7.5.5).

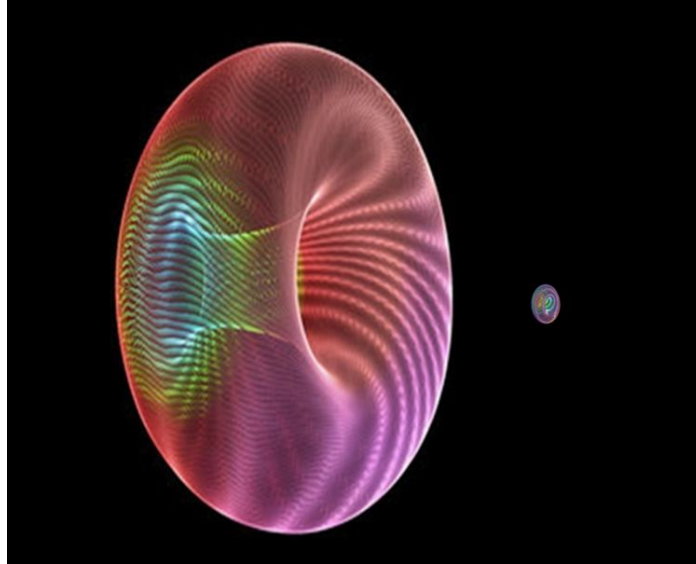


Fig. 7.5.5. Illustration of the comparative dimensions of aquatic «neutrino» and electron «neutrino», the radius of the neck which differ by 7 orders of magnitude

«Neutrino» is able to interact with other «particles» mainly when the core of these «particles» fall into the neck of the toroidal-helical vortex or double toroidal-helical vortex, because it is in this place that vacuum flows are most concentrated and intense. Therefore, the probability of interaction of «neutrinos» with other particles P_n is proportional to the sectional area of its neck S_n .

For example, the probability of interaction of the electron «neutrino» can be assessed by expression of

For example, the probability of interaction of an electron «neutrino» with cores of other elementary «particles» can be estimated by the expression

$$P_{en} \sim S_{en} = A_e \pi r_{en}^2, \quad (7.5.6)$$

were A_e is the coefficient of efficiency of interaction of the electron «neutrino» with cores of other «particles».

Similarly, the probability of aquatic «neutrino» interaction is estimated by the expression

$$P_{wn} \sim S_{en} = A_w \pi r_{en}^2. \quad (7.5.7)$$

where A_w is the coefficient of efficiency of interaction of aquatic «neutrino» with cores of other «particles».

Therefore, under the condition $A_w \approx A_e$, a aquatic «neutrino» can more often interact with the cores of other «particles» than the electron «neutrino» by about 14 orders of magnitude, because:

$$S_{wn}/S_{en} = r_{wn}^2/r_{en}^2 \approx 10^{-12}/10^{-26} \sim 10^{14}. \quad (7.5.8)$$

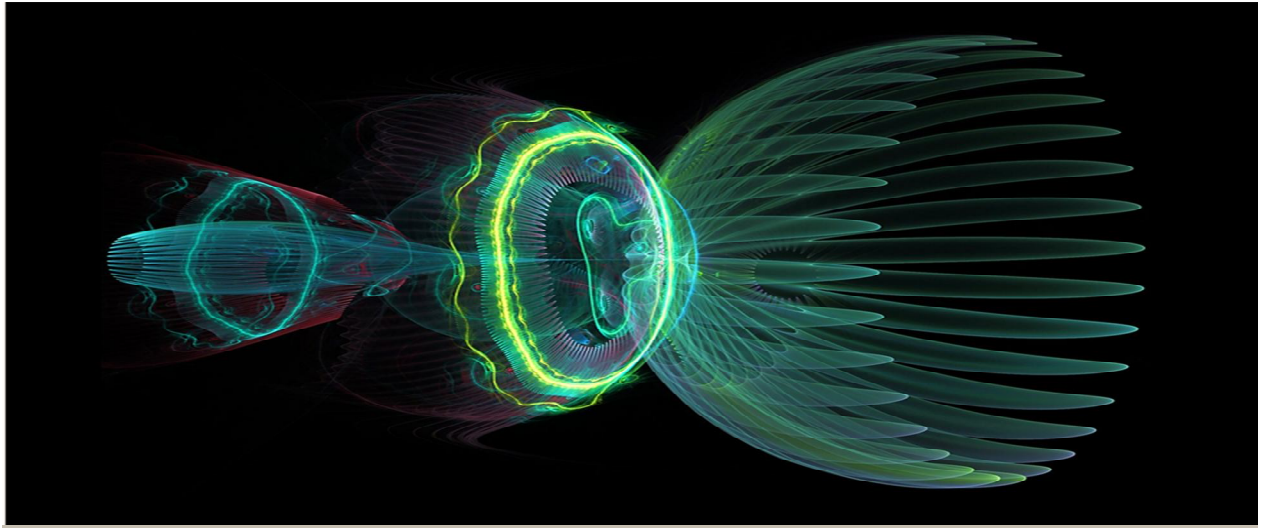


Fig. 7.5.5a. Fractal illustration of the collision of the core of an elementary "particle" with the neck of a «neutrino»

Thus, aquatic «neutrinos» (if their existence is confirmed) can be more effectively used for the development of new (possibly superluminal) data transmission technologies. Note, however, that the double (subcont - antisubcont) toroidal-helical vortices can otherwise affect the substance than single (subcont or antisubcont) toroidal-helical vortices.

Another possible method of obtaining macroscopic «neutrino» is associated with a toroidal inductor (Figure 7.5.6). The magnetic field of a toroidal coil with a direct current resembles a toroidal-helical vortex. From the point of view of an Alsigna it also is the closed intra-vacuum currents. It is possible that if such a coil with a direct current is forced to move progressively, and then sharply slow down, then a coiled «neutri-

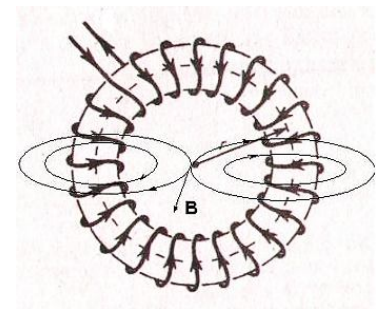
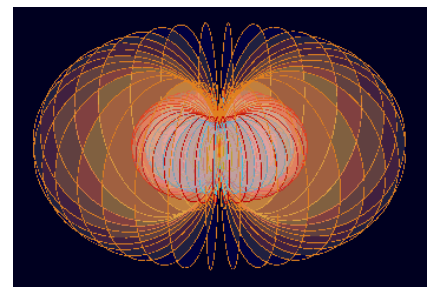


Fig. 7.5.6. Toroidal magnetic field of a toroidal coil with a direct current

no» (i.e. a toroidal-helical vortex consisting of closed intra-vacuum currents of macroscopic scale) can break from such a coil. It should be expected that the initial radius of the neck of such a coiled «neutrino» is commensurate with the radius of the toroidal coil (Figure 7.5.7).



Fig. 7.5.7. The Algebra of Signatures does not impose restrictions on the size of toroidal vacuum formations, which are conventionally called «neutrino»

7.6 Excited States of «neutrinos»

We have considered above the simplest versions of «neutrinos» that have kind of toroidal-helical vortices (Figure 7.4.2).

In Chapters 3 and 4 the foundations of statistical and quantum geometry (stochastic metaphysics) were laid, and it was shown that the averaged metric-dynamic states of stable vacuum formations depend not only on the balance between the deformations of the local parts of the inner 2^3 - $\lambda_{m,n}$ -vacuum region and their accelerated flows, but also on the degree of excitation of their chaotic motion.

In this paper, we will not deal in detail with various aspects of stochastic metaphysics, because this should be devoted to a separate extensive study. Note only that the «neutrinos» as well as the «electron's» core (see Chapters 3 and 4) can be found in various excited states with different averaged configurations of the metric-dynamic structure of the intra-vacuum layer. In this case, each level of the excited state of the "neutrino" can correspond to a unique averaged configuration of the vacuum layers and the interlacing of accelerated intra-vacuum flows (Figure 7.6.1).

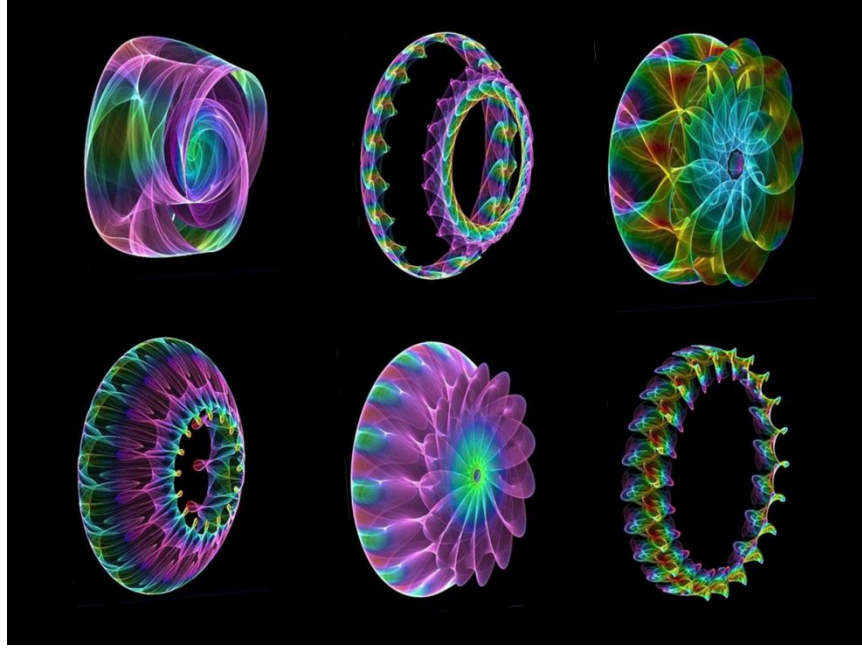


Fig. 7.6.1. Fractal illustration of different possible configurations of the averaged excited states of «neutrinos»

It is possible that muon «neutrinos» and τ -lepton «neutrinos» are respectively the first and second excited states of electron «neutrinos».

It is also necessary to consider such types of perturbation of a toroidal-helical vortex (for example, an electron «neutrino») as an averaged precession of its rotation axis around the z direction of motion (Figure 7.6.2).

Quantum effects associated with the averaged precession of the «neutrino» axis of rotation can be described by analogy with the description of the precession of the axis of rotation of the core of the moving «electron» (*see § 6.12*).

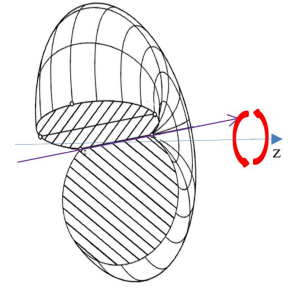


Fig. 7.6.2. Illustration of the precession of the rotation axis of the toroidal-helical vortex around the direction z of its motion

7.7 Protonic «neutrino»

Metric-dynamic model of resting «proton» (2.9.21) with topological configuration (2.9.9)

$$\begin{aligned} d_k^+ (+ + + -) \\ u_3^- (- + - +) \\ u_r^- (- - + +) \\ p_l^+ (- + + +)_+ \end{aligned} \quad (7.7.1)$$

taking into account that in the neighborhood of its core $r_5 \gg r_6$ can be represented in a simplified form

«PROTON»

(7.7.2)

on average "concave" stable multilayer vacuum formation

(Figure 2.9.1), with the total signature

$$(+++ -) + (-+ -) + (- - +) = \mathbf{(- + + +)}$$

consisting of:

d_r^+ -«quark»

(7.7.3)

with signature

$$(+++ -)$$

The outer shell of the d_r^+ -«quark»

in the interval $[\sim 10^{-13} \text{ cm}, \sim 10^{18} \text{ cm}]$

$$ds_1^{(+++)^2} = \left(1 - \frac{r_6}{r}\right) c^2 dt^2 + \frac{dr^2}{\left(1 - \frac{r_6}{r}\right)} + r^2 d\theta^2 - r^2 \sin^2 \theta d\varphi^2,$$

$$ds_2^{(+++)^2} = \left(1 + \frac{r_6}{r}\right) c^2 dt^2 + \frac{dr^2}{\left(1 + \frac{r_6}{r}\right)} + r^2 d\theta^2 - r^2 \sin^2 \theta d\varphi^2;$$

The core of the d_r^+ -«quark»

in the interval $[\sim 10^{-24} \text{ cm}, \sim 10^{-13} \text{ cm}]$

$$ds_1^{(+++)^2} = \left(1 - \frac{r_7}{r} + \frac{r^2}{r_6^2}\right) c^2 dt^2 + \frac{dr^2}{\left(1 - \frac{r_7}{r} + \frac{r^2}{r_6^2}\right)} + r^2 d\theta^2 - r^2 \sin^2 \theta d\varphi^2,$$

$$ds_2^{(+++)^2} = \left(1 + \frac{r_7}{r} - \frac{r^2}{r_6^2}\right) c^2 dt^2 + \frac{dr^2}{\left(1 + \frac{r_7}{r} - \frac{r^2}{r_6^2}\right)} + r^2 d\theta^2 - r^2 \sin^2 \theta d\varphi^2,$$

$$ds_3^{(+++)^2} = \left(1 - \frac{r_7}{r} - \frac{r^2}{r_6^2}\right) c^2 dt^2 + \frac{dr^2}{\left(1 - \frac{r_7}{r} - \frac{r^2}{r_6^2}\right)} + r^2 d\theta^2 - r^2 \sin^2 \theta d\varphi^2,$$

$$ds_4^{(+++)^2} = \left(1 + \frac{r_7}{r} + \frac{r^2}{r_6^2}\right) c^2 dt^2 + \frac{dr^2}{\left(1 + \frac{r_7}{r} + \frac{r^2}{r_6^2}\right)} + r^2 d\theta^2 - r^2 \sin^2 \theta d\varphi^2;$$

The scope of the d_r^+ -«quark»

in the interval $[0, \infty]$

$$ds_5^{(+++)^2} = c^2 dt^2 + dr^2 + r^2 d\theta^2 - r^2 \sin^2 \theta d\varphi^2.$$

u_g^- -«antiquark»
 with signature
 $(-+-+)$
 which consists of:

(7.7.4)

The outer shell of the u_g^- -«antiquark»

in the interval $[\sim 10^{-13} \text{ cm}, \sim 10^{18} \text{ cm}]$

$$ds_1^{(-++)^2} = -\left(1 - \frac{r_6}{r}\right) c^2 dt^2 + \frac{dr^2}{\left(1 - \frac{r_6}{r}\right)} - r^2 d\theta^2 + r^2 \sin^2 \theta d\varphi^2,$$

$$ds_2^{(-++)^2} = -\left(1 + \frac{r_6}{r}\right) c^2 dt^2 + \frac{dr^2}{\left(1 + \frac{r_6}{r}\right)} - r^2 d\theta^2 + r^2 \sin^2 \theta d\varphi^2;$$

The core of the u_g^- -«antiquark»

in the interval $[\sim 10^{-24} \text{ cm}, \sim 10^{-13} \text{ cm}]$

$$ds_1^{(-++)^2} = -\left(1 - \frac{r_7}{r} + \frac{r^2}{r_6^2}\right) c^2 dt^2 + \frac{dr^2}{\left(1 - \frac{r_7}{r} + \frac{r^2}{r_6^2}\right)} - r^2 d\theta^2 + r^2 \sin^2 \theta d\varphi^2,$$

$$ds_2^{(-++)^2} = -\left(1 + \frac{r_7}{r} - \frac{r^2}{r_6^2}\right) c^2 dt^2 + \frac{dr^2}{\left(1 + \frac{r_7}{r} - \frac{r^2}{r_6^2}\right)} - r^2 d\theta^2 + r^2 \sin^2 \theta d\varphi^2,$$

$$ds_3^{(-++)^2} = -\left(1 - \frac{r_7}{r} - \frac{r^2}{r_6^2}\right) c^2 dt^2 + \frac{dr^2}{\left(1 - \frac{r_7}{r} - \frac{r^2}{r_6^2}\right)} - r^2 d\theta^2 + r^2 \sin^2 \theta d\varphi^2,$$

$$ds_4^{(-++)^2} = -\left(1 + \frac{r_7}{r} + \frac{r^2}{r_6^2}\right) c^2 dt^2 + \frac{dr^2}{\left(1 + \frac{r_7}{r} + \frac{r^2}{r_6^2}\right)} - r^2 d\theta^2 + r^2 \sin^2 \theta d\varphi^2;$$

The scope of the u_g^- -«antiquark»

in the interval $[0, \infty]$

$$ds_5^{(-++)^2} = -c^2 dt^2 + dr^2 - r^2 d\theta^2 + r^2 \sin^2 \theta d\varphi^2.$$

$$\begin{aligned} & \mathbf{u_b^- - \langle\langle antiquark \rangle\rangle} \\ & \text{with signature} \\ & (- - + +) \end{aligned} \quad (7.7.5)$$

The outer shell of the u_b^- -«antiquark»
in the interval $[\sim 10^{-13} \text{ cm}, \sim 10^{18} \text{ cm}]$

$$ds_1^{(---+)^2} = -\left(1 - \frac{r_6}{r}\right) c^2 dt^2 - \frac{dr^2}{\left(1 - \frac{r_6}{r}\right)} + r^2 d\theta^2 + r^2 \sin^2 \theta d\varphi^2,$$

$$ds_2^{(---+)^2} = -\left(1 + \frac{r_6}{r}\right) c^2 dt^2 - \frac{dr^2}{\left(1 + \frac{r_6}{r}\right)} + r^2 d\theta^2 + r^2 \sin^2 \theta d\varphi^2,$$

The core of the u_b^- -«antiquark»
in the interval $[\sim 10^{-24} \text{ cm}, \sim 10^{-13} \text{ cm}]$

$$ds_1^{(---+)^2} = -\left(1 - \frac{r_7}{r} + \frac{r^2}{r_6^2}\right) c^2 dt^2 - \frac{dr^2}{\left(1 - \frac{r_7}{r} + \frac{r^2}{r_6^2}\right)} + r^2 d\theta^2 + r^2 \sin^2 \theta d\varphi^2,$$

$$ds_2^{(---+)^2} = -\left(1 + \frac{r_7}{r} - \frac{r^2}{r_6^2}\right) c^2 dt^2 - \frac{dr^2}{\left(1 + \frac{r_7}{r} - \frac{r^2}{r_6^2}\right)} + r^2 d\theta^2 + r^2 \sin^2 \theta d\varphi^2,$$

$$ds_3^{(---+)^2} = -\left(1 - \frac{r_7}{r} - \frac{r^2}{r_6^2}\right) c^2 dt^2 - \frac{dr^2}{\left(1 - \frac{r_7}{r} - \frac{r^2}{r_6^2}\right)} + r^2 d\theta^2 + r^2 \sin^2 \theta d\varphi^2,$$

$$ds_4^{(---+)^2} = -\left(1 + \frac{r_7}{r} + \frac{r^2}{r_6^2}\right) c^2 dt^2 - \frac{dr^2}{\left(1 + \frac{r_7}{r} + \frac{r^2}{r_6^2}\right)} + r^2 d\theta^2 + \sin^2 \theta d\varphi^2,$$

The scope of the u_b^- -«antiquark»
in the interval $[0, \infty]$:

$$ds_5^{(---+)^2} = -c^2 dt^2 - dr^2 + r^2 d\theta^2 + r^2 \sin^2 \theta d\varphi^2,$$

were

$r_7 \sim 5.8 \cdot 10^{-24} \text{ cm}$: \sim core of an «protoquark» {see hierarchy (2.6.20)}.

$r_6 \sim 1.7 \cdot 10^{-13} \text{ cm}$: \sim core of an elementary «particle» (in particular, «electron»);

If the «proton» begins to move relative to $2^3\text{-}\lambda_{-11,-16}$ -vacuum region, the deformation of which he is, then in its outer shell is induced toroidal-helical rotational motion similar to the movement in the outer shell of the moving «electron», but much more complex (Figure 7.7.1).

The complexity of the rotation of the outer shell of the moving «proton» is due to the fact that it is the result of the imposition of three intertwined metric layers $2^3\text{-}\lambda_{-11,-16}$ -vacuum region with different signatures (topologies).

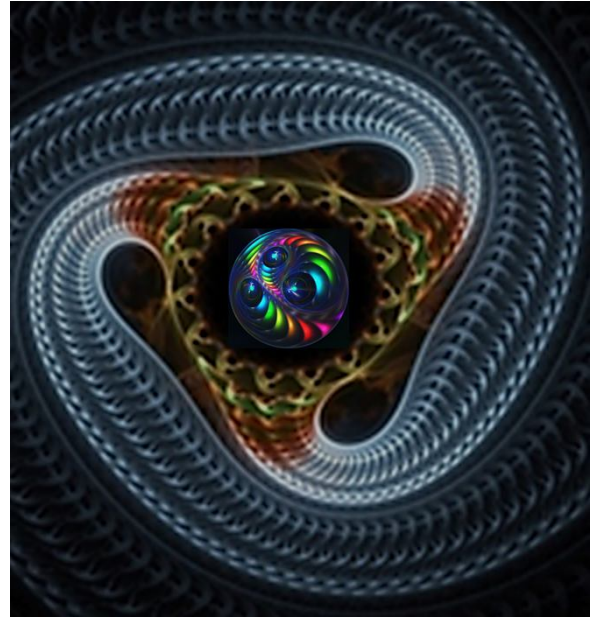


Fig. 7.7.1. Illustrations of the topological configuration of the outer shell and the «proton's» core

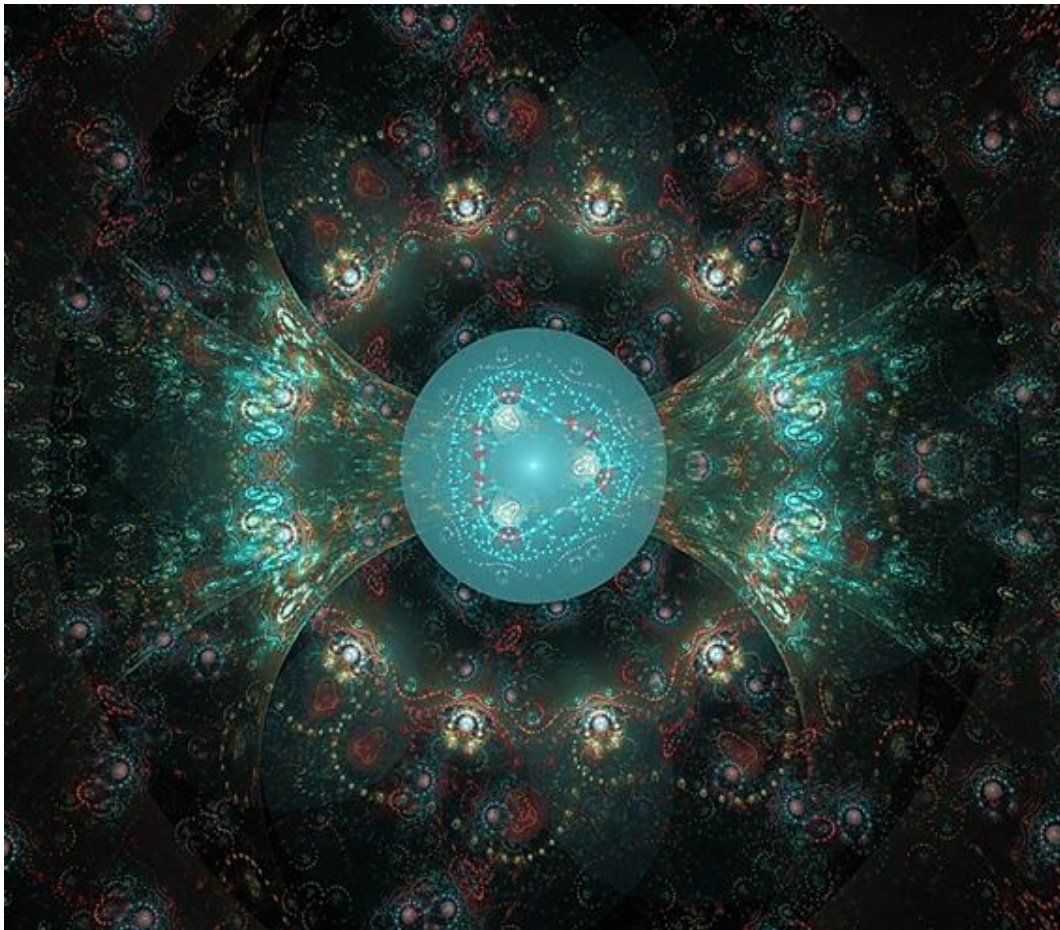


Fig. 7.7.2. Illustration of the core and outer shell of the resting «proton»

In the framework of the Alsigna, the metric-dynamic model of the outer shell of the «proton», moving at a constant speed V_z , is given by the following set of metrics [similar to metrics (7.1.1) through (7.1.4), but with other signatures]:

**Outer shell of the moving
«PROTON»** (7.7.6)

with the total signature

$$(+ + + -) + (- + - +) + (- - + +) = (- + + +)$$

consisting of:

The outer shell of the moving d_r^+ -«quark» (7.7.7)

with signature $(+ + + -)$

in the interval $[\sim 10^{-13} \text{ cm}, \sim 10^{18} \text{ cm}]$

$$ds_1^{(-a)2} = \left(1 - \frac{r_6 r}{r^2 + a_p^2 \cos^2 \theta}\right) c^2 dt^2 + \frac{r^2 + a_p^2 \cos^2 \theta}{r^2 + a_p^2 - r r_6} dr^2 + (r^2 + a_p^2 \cos^2 \theta) d\theta^2 -$$

– a_1 -subcont;

$$- \left(r^2 + a_p^2 + \frac{r_6 r a_p^2 \sin^2 \theta}{r^2 + a_p^2 \cos^2 \theta}\right) \sin^2 \theta d\varphi^2 - \frac{2 r_6 r a_p}{r^2 + a_p^2 \cos^2 \theta} \sin^2 \theta d\varphi c dt.$$

$$ds_1^{(-b)2} = \left(1 + \frac{r_6 r}{r^2 + a_p^2 \cos^2 \theta}\right) c^2 dt^2 + \frac{r^2 + a_p^2 \cos^2 \theta}{r^2 + a_p^2 + r r_6} dr^2 + (r^2 + a_p^2 \cos^2 \theta) d\theta^2 -$$

– b_1 -subcont

$$- \left(r^2 + a_p^2 - \frac{r_6 r a_p^2 \sin^2 \theta}{r^2 + a_p^2 \cos^2 \theta}\right) \sin^2 \theta d\varphi^2 - \frac{2 r_6 r a_p}{r^2 + a_p^2 \cos^2 \theta} \sin^2 \theta d\varphi c dt.$$

The outer shell of the moving u_g^- -«antiquark» (7.7.8)

with signature $(- + - +)$

in the interval $[\sim 10^{-13} \text{ cm}, \sim 10^{18} \text{ cm}]$

$$ds_2^{(-a)2} = - \left(1 - \frac{r_6 r}{r^2 + a_p^2 \cos^2 \theta}\right) c^2 dt^2 + \frac{r^2 + a_p^2 \cos^2 \theta}{r^2 + a_p^2 - r r_6} dr^2 - (r^2 + a_p^2 \cos^2 \theta) d\theta^2 +$$

– a_2 -antisubcont,

$$+ \left(r^2 + a_p^2 + \frac{r_6 r a_p^2 \sin^2 \theta}{r^2 + a_p^2 \cos^2 \theta}\right) \sin^2 \theta d\varphi^2 - \frac{2 r_6 r a_p}{r^2 + a_p^2 \cos^2 \theta} \sin^2 \theta d\varphi c dt.$$

$$ds_2^{(-b)2} = - \left(1 + \frac{r_6 r}{r^2 + a_p^2 \cos^2 \theta}\right) c^2 dt^2 + \frac{r^2 + a_p^2 \cos^2 \theta}{r^2 + a_p^2 + r r_6} dr^2 - (r^2 + a_p^2 \cos^2 \theta) d\theta^2 -$$

– b_2 -antisubcont

$$+ \left(r^2 + a_p^2 - \frac{r_6 r a_p^2 \sin^2 \theta}{r^2 + a_p^2 \cos^2 \theta}\right) \sin^2 \theta d\varphi^2 - \frac{2 r_6 r a_p}{r^2 + a_p^2 \cos^2 \theta} \sin^2 \theta d\varphi c dt.$$

The outer shell of the moving u_g^- -«antiquark»

(7.7.9)

with signature $(- - + +)$
in the interval $[\sim 10^{-13} \text{ cm}, \sim 10^{18} \text{ cm}]$

$$ds_3^{(-a)^2} = - \left(1 - \frac{r_6 r}{r^2 + a_p^2 \cos^2 \theta} \right) c^2 dt^2 - \frac{r^2 + a_p^2 \cos^2 \theta}{r^2 + a_p^2 - r r_6} dr^2 + (r^2 + a_p^2 \cos^2 \theta) d\theta^2 +$$

– a_3 -antisubcont;

$$+ \left(r^2 + a_p^2 + \frac{r_6 r a_p^2 \sin^2 \theta}{r^2 + a_p^2 \cos^2 \theta} \right) \sin^2 \theta d\varphi^2 - \frac{2 r_6 r a_p}{r^2 + a_p^2 \cos^2 \theta} \sin^2 \theta d\varphi c dt$$

$$ds_3^{(-b)^2} = - \left(1 + \frac{r_6 r}{r^2 + a_p^2 \cos^2 \theta} \right) c^2 dt^2 - \frac{r^2 + a_p^2 \cos^2 \theta}{r^2 + a_p^2 + r r_6} dr^2 + (r^2 + a_p^2 \cos^2 \theta) d\theta^2 +$$

– b_3 -antisubcont

$$+ \left(r^2 + a_p^2 - \frac{r_6 r a_p^2 \sin^2 \theta}{r^2 + a_p^2 \cos^2 \theta} \right) \sin^2 \theta d\varphi^2 - \frac{2 r_6 r a_p}{r^2 + a_p^2 \cos^2 \theta} \sin^2 \theta d\varphi c dt$$

The scope of the moving u_b^- -«antiquark»

(7.7.10)

with a total signature
 $(+ + + -) + (- + - +) + (- - + +) = (- + + +)$
in the interval $[0, \infty]$:

$$ds_4^{(++++)^2} = ds_4^{(++++)^2} + ds_4^{(---+)^2} + ds_4^{(----)^2},$$

where

$$ds_4^{(++++)^2} = c^2 dt^2 + \frac{\rho_p^2 dr^2}{r^2 + a_p^2} + \rho_p^2 d\theta^2 - (r^2 + a_p^2) \sin^2 \theta d\varphi^2,$$

$$ds_4^{(---+)^2} = -c^2 dt^2 + \frac{\rho_p^2 dr^2}{r^2 + a_p^2} - \rho_p^2 d\theta^2 + (r^2 + a_p^2) \sin^2 \theta d\varphi^2,$$

$$ds_4^{(----)^2} = -c^2 dt^2 - \frac{\rho_p^2 dr^2}{r^2 + a_p^2} + \rho_p^2 d\theta^2 + (r^2 + a_p^2) \sin^2 \theta d\varphi^2,$$

where $\rho_p^2 = r^2 + a_p^2 \cos^2 \theta$;

$r_6 \sim 1.7 \cdot 10^{-13} \text{ cm}$ is the radius of the core of «proton» is approximately equal to the radius of the core of an «electron»;

$a_p = r_6 \frac{V_z}{2c}$ is the parameter of ellipticity of «proton», moving with a constant velocity V_z (in

the z axis direction) as a single vacuum formation relative to resting $2^3\text{-}\lambda_{11,16}$ -vacuum region, of which he is consists.

It is obvious that the inert properties of such a stable vacuum formation (7.7.6) should be much more noticeable than the inert properties of the moving «electron».

Similarly, the outer shell of the «antiproton» (i.e., on average, a convex stable multilayered vacuum formation) is arranged, which consists of the outer shells of three "quarks", for example, with signatures (2.9.13)

$$\begin{array}{l} d_3^- (- - + -) \\ u_r^+ (+ + - -) \\ u_k^+ (+ - - +) \\ p_2^- (+ - - -)_+ \end{array} \quad (7.7.11)$$

That is, the outer shell of the «antiproton» is described by metrics of the form (7.7.7) through (7.7.10), but with signatures (7.7.11).

By analogy with (7.4.1) through (7.4.3), the initial state of the «protonic» neutrino (i.e., immediately after it breaks from the «proton's» core) can be specified by the following set of metrics:

The initial state of the protonic «neutrino» (7.7.12)

$$\begin{array}{l} \text{with total signature} \\ (+ + + -) + (- + - +) + (- - + +) = (- + + +) \\ \text{in the interval } [\sim 10^{-13} \text{ cm}, \sim 10^{18} \text{ cm}] \end{array}$$

$$\begin{aligned} ds_1^{(++++a)2} = & c^2 dt^2 + \frac{r^2 + a_p^2 \cos^2 \theta}{r^2 + a_p^2 - rr_6} dr^2 + (r^2 + a_p^2 \cos^2 \theta) d\theta^2 - \\ & - \left(r^2 + a_p^2 + \frac{r_6 r a_p^2 \sin^2 \theta}{r^2 + a_p^2 \cos^2 \theta} \right) \sin^2 \theta d\varphi^2 - \frac{2r_6 r a_p}{r^2 + a_p^2 \cos^2 \theta} \sin^2 \theta d\varphi c dt \end{aligned} \quad \begin{array}{l} - a_1\text{-subcont} \\ (7.7.13) \end{array}$$

$$\begin{aligned} ds_1^{(++++b)2} = & c^2 dt^2 + \frac{r^2 + a_p^2 \cos^2 \theta}{r^2 + a_p^2 + rr_6} dr^2 + (r^2 + a_p^2 \cos^2 \theta) d\theta^2 - \\ & - \left(r^2 + a_p^2 - \frac{r_6 r a_p^2 \sin^2 \theta}{r^2 + a_p^2 \cos^2 \theta} \right) \sin^2 \theta d\varphi^2 - \frac{2r_6 r a_p}{r^2 + a_p^2 \cos^2 \theta} \sin^2 \theta d\varphi c dt \end{aligned} \quad \begin{array}{l} - b_1\text{-subcont} \\ (7.7.14) \end{array}$$

$$\begin{aligned} ds_2^{(---+a)2} = & -c^2 dt^2 + \frac{r^2 + a_p^2 \cos^2 \theta}{r^2 + a_p^2 - rr_6} dr^2 - (r^2 + a_p^2 \cos^2 \theta) d\theta^2 + \\ & + \left(r^2 + a_p^2 + \frac{r_6 r a_p^2 \sin^2 \theta}{r^2 + a_p^2 \cos^2 \theta} \right) \sin^2 \theta d\varphi^2 - \frac{2r_6 r a_p}{r^2 + a_p^2 \cos^2 \theta} \sin^2 \theta d\varphi c dt \end{aligned} \quad \begin{array}{l} - a_2\text{-antisubcont}, \\ (7.7.15) \end{array}$$

$$\begin{aligned} ds_2^{(---+b)2} = & -c^2 dt^2 + \frac{r^2 + a_p^2 \cos^2 \theta}{r^2 + a_p^2 + rr_6} dr^2 - (r^2 + a_p^2 \cos^2 \theta) d\theta^2 - \\ & + \left(r^2 + a_p^2 - \frac{r_6 r a_p^2 \sin^2 \theta}{r^2 + a_p^2 \cos^2 \theta} \right) \sin^2 \theta d\varphi^2 - \frac{2r_6 r a_p}{r^2 + a_p^2 \cos^2 \theta} \sin^2 \theta d\varphi c dt \end{aligned} \quad \begin{array}{l} - b_2\text{-antisubcont} \\ (7.7.16) \end{array}$$

$$ds_3^{(--++a)^2} = -c^2 dt^2 - \frac{r^2 + a_p^2 \cos^2 \theta}{r^2 + a_p^2 - rr_6} dr^2 + (r^2 + a_p^2 \cos^2 \theta) d\theta^2 +$$

$$+ \left(r^2 + a_p^2 + \frac{r_6 r a_p^2 \sin^2 \theta}{r^2 + a_p^2 \cos^2 \theta} \right) \sin^2 \theta d\varphi^2 - \frac{2r_6 r a_p}{r^2 + a_p^2 \cos^2 \theta} \sin^2 \theta d\varphi c dt$$

– a_3 -antisubcont (7.7.17)

$$ds_3^{(--++b)^2} = -c^2 dt^2 - \frac{r^2 + a_p^2 \cos^2 \theta}{r^2 + a_p^2 + rr_6} dr^2 + (r^2 + a_p^2 \cos^2 \theta) d\theta^2 +$$

$$+ \left(r^2 + a_p^2 - \frac{r_6 r a_p^2 \sin^2 \theta}{r^2 + a_p^2 \cos^2 \theta} \right) \sin^2 \theta d\varphi^2 - \frac{2r_6 r a_p}{r^2 + a_p^2 \cos^2 \theta} \sin^2 \theta d\varphi c dt.$$

– b_3 -antisubcont. (7.7.18)

The scope of the initial state of protonic «neutrino» (7.7.19)

with a total signature
 $(+++ -) + (-+ -) + (- - +) = (- + +)$
in the interval $[0, \infty]$

$$ds_4^{(++++)^2} = ds_4^{(++++)^2} + ds_4^{(---+)^2} + ds_4^{(--++)^2},$$

where

$$ds_4^{(++++)^2} = c^2 dt^2 + \frac{\rho_p^2 dr^2}{r^2 + a_p^2} + \rho_p^2 d\theta^2 - (r^2 + a_p^2) \sin^2 \theta d\varphi^2,$$

$$ds_4^{(---+)^2} = -c^2 dt^2 + \frac{\rho_p^2 dr^2}{r^2 + a_p^2} - \rho_p^2 d\theta^2 + (r^2 + a_p^2) \sin^2 \theta d\varphi^2,$$

$$ds_4^{(--++)^2} = -c^2 dt^2 - \frac{\rho_p^2 dr^2}{r^2 + a_p^2} + \rho_p^2 d\theta^2 + (r^2 + a_p^2) \sin^2 \theta d\varphi^2,$$

where $\rho_p^2 = r^2 + a_p^2 \cos^2 \theta$; (7.7.20)

$r_6 \sim 1.7 \cdot 10^{-13}$ cm is the radius of the core of «proton» is approximately equal to the radius of the core of an «electron»;

$a_p = r_6 \frac{V_z}{2c}$ is the parameter of ellipticity of «proton», moving with a constant velocity V_z (in

the z axis direction) as a single vacuum formation relative to resting 2^3 - $\lambda_{-11,-16}$ -vacuum region, of which he is consists.

The initial state of the antiproton «neutrino» can be specified by a set of metrics of the form (7.7.13) through (7.7.20), but with signatures, for example (7.7.11).

By analogy with (7.4.1) through (7.4.3), the metric-dynamic model the final state of the protonic «neutrino» and antiprotonic «neutrino» in the framework Alsina have the form:

The protonic «neutrino» (7.7.21)

with a total signature

$$(+++ -) + (-+- +) + (--+ +) = (-+++)$$

in the interval $[0, \infty]$:

$$ds^{(+++-)^2} = c^2 dt^2 + \frac{r^2 + a_p^2 \cos^2 \theta}{r^2 + a_p^2} dr^2 + (r^2 + a_p^2 \cos^2 \theta) d\theta^2 - (r^2 + a_p^2) \sin^2 \theta d\varphi^2 \quad (7.7.22)$$

$$ds^{(-++-)^2} = -c^2 dt^2 + \frac{r^2 + a_p^2 \cos^2 \theta}{r^2 + a_p^2} dr^2 - (r^2 + a_p^2 \cos^2 \theta) d\theta^2 + (r^2 + a_p^2) \sin^2 \theta d\varphi^2 \quad (7.7.23)$$

$$ds^{(--+-)^2} = -c^2 dt^2 - \frac{r^2 + a_p^2 \cos^2 \theta}{r^2 + a_p^2} dr^2 + (r^2 + a_p^2 \cos^2 \theta) d\theta^2 + (r^2 + a_p^2) \sin^2 \theta d\varphi^2; \quad (7.7.24)$$

The scope of the protonic «neutrino» (7.7.25)

with a total signature

$$(+++ -) + (-+- +) + (--+ +) = (-+++)$$

in the interval $[0, \infty]$:

$$ds^{(-)^2} = -c^2 dt^2 + dr^2 + r^2 d\theta^2 + r^2 \sin^2 \theta d\varphi^2.$$

The antiprotonic «neutrino» (7.7.26)

with a total signature

$$(-+- -) + (++- -) + (+-- +) = (+---)$$

in the interval $[0, \infty]$:

$$ds^{(---)^2} = -c^2 dt^2 - \frac{r^2 + a_p^2 \cos^2 \theta}{r^2 + a_p^2} dr^2 + (r^2 + a_p^2 \cos^2 \theta) d\theta^2 - (r^2 + a_p^2) \sin^2 \theta d\varphi^2 \quad (7.7.27)$$

$$ds^{(++-)^2} = c^2 dt^2 + \frac{r^2 + a_p^2 \cos^2 \theta}{r^2 + a_p^2} dr^2 - (r^2 + a_p^2 \cos^2 \theta) d\theta^2 - (r^2 + a_p^2) \sin^2 \theta d\varphi^2 \quad (7.7.28)$$

$$ds^{(+--)^2} = c^2 dt^2 - \frac{r^2 + a_p^2 \cos^2 \theta}{r^2 + a_p^2} dr^2 - (r^2 + a_p^2 \cos^2 \theta) d\theta^2 + (r^2 + a_p^2) \sin^2 \theta d\varphi^2; \quad (7.7.29)$$

The scope of the antiprotonic «neutrino» (7.7.30)

with a total signature

$$(-+- -) + (++- -) + (+-- +) = (+---)$$

in the interval $[0, \infty]$:

$$ds^{(-)^2} = c^2 dt^2 - dr^2 - r^2 d\theta^2 - r^2 \sin^2 \theta d\varphi^2.$$

7.8 "Kelyphosons" and "rozosons"

The Algebra of Signature (Alsigna) observes two classes of stable vacuum formations.

First class stable formations have a pronounced enclosed cores, surrounded by a *rakya* (multi-layer shell) and inner nucleolus (or many inner nucleoli) inside the core (Figure 7.8.1)



Fig. 7.8.1. Fractal illustration of a particle-like vacuum structures ("**kelyphosons**"), having pronounced an enclosed core, surrounded by a *rakya* (multilayer shell), and having an inner nucleolus (or nucleoli).

The second class of stable vacuum formations is always composed of a very complex node, woven from intra-vacuum currents, which in turn are balanced by ornate deformations (Figure 7.4.2 and 7.8.2).

Such vacuum formations remain stable due to the constant infinitely complex closed motion of its layers. This is a kind of soliton, but with movements and deformations closed on themselves, often with the flow of intra-vacuum currents from layer to layer, twisted into hybrids of spirals and Möbius bands.



Fig. 7.8.2. Fractal illustrations of various stable self-closed interlacing intra-vacuum currents, which are called "**rozosons**"

The first class of particle-like vacuum formations (Figure 7.8.1) we will call "**kelyphosons**" from the Greek word κέλυφος (shell), and the second type of vacuum formations of a soliton-like type (Figure 7.8.2) will be called the "**rozosons**" from the Greek word **πόζος** (node). (This terminology was proposed by an editor.)

All types of "neutrinos" discussed in this chapter are the representatives of "**rozosons**", i.e. confined soliton-like vacuum structures.

According to Alsigna, the study of metric-dynamic and quantum-geometric properties of different varieties of "neutrino" is one of the first steps towards the study of this class of entities that inhabit the space around us.

7.9 Conclusion to Chapter 7

This article describes only some aspects of the metric-dynamic structure of the local vacuum formation, which Alsigna calls «neutrinos».

The metric-dynamic properties of different varieties of «neutrino» should be the subject of a separate extensive study, which could lead to the development of various advanced vacuum technologies.

In particular, there were no issues related to the collision of two «neutrinos» (Figure 7.9.1), and many other aspects of their interaction have not been investigated.

An interesting problem is the organization of "neutrino" motion along a circular trajectory to create continuous data carriers, etc.

Note also that the article of the metric-dynamic model only microscopic «neutrino». However, let us recall that the mathematical apparatus of the Algebra of signature is universal and suitable for describing the metric-dynamic properties of vacuum formations of various scales.

However, let us recall that the mathematical apparatus of the Algebra of Signature is universal and suitable for describing the metric-dynamic properties of vacuum formations of various scales.

If, in all metrics of this chapter and the previous chapter, Chapter 6, we substitute any other radius from the hierarchy (2.6.20) -- for example, the radius of the «planet's» (or «star's») core $r_4 \sim 1.4 \cdot 10^8$ cm, or the radius of the «galaxy's» core $r_3 \sim 4 \cdot 10^{18}$ cm -- for the radius of the «electron's» (or «proton's») core $r_6 \sim 1.7 \cdot 10^{-13}$ cm, we get (continuing the examples) a description of the toroidal-helical fields' vacuum intensity of the moving «planet» («star») (Figure 7.9.2), or the vacuum induction of the mobile «galaxy» (Figure 7.9.3), respectively.

Thus, in the framework of Alsigna can be raised about the possibility of detection and generation of «neutrino» planetary and galactic scale.

It is possible that, for example, a planetary «neutrino» can fly off the planet in the form of a toroidal-helical vortex (i.e., a closed magnetic field), when it collides with another planet, or with a large comet.

Similarly, the magnetic field of a sharply stopped «galaxy» can fly off it and form a toroidal-helical vortex («neutrino») of galactic scale.



Fig. 7.9.1. Fractal illustration of collision of two «neutrinos»

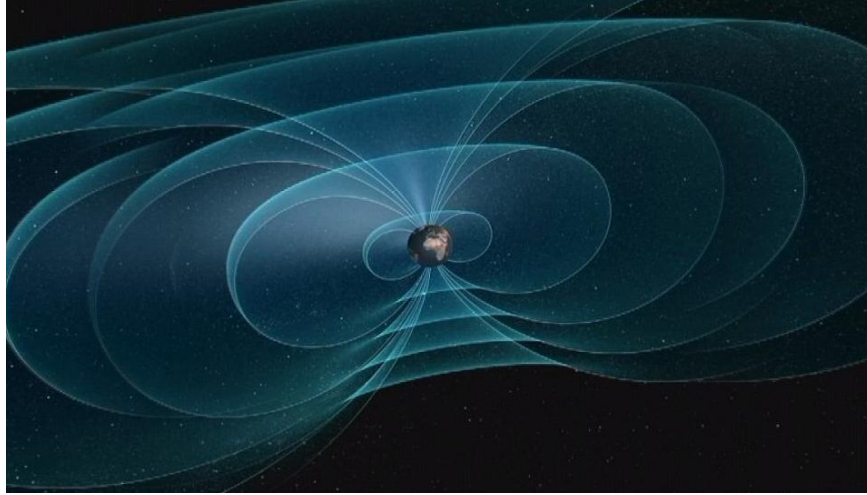


Fig. 7.9.2. Illustration of a toroidal-helical field of vacuum induction (i.e., magnetic field) induced around a moving and rotating planet (or star) (art. <http://static.euronews.com>)



Fig. 7.8.3. Illustration of the toroidal-helical field of vacuum induction (i.e., magnetic field) induced around a moving and rotating galaxy (<https://ic.pics.livejournal.com>)